

**Impacts of Drought and 40% Throughfall Reduction on  
Water Relations of a Longleaf Pine Stand**

by

Michael Roldan Ramirez, Jr.

A thesis submitted to the Graduate Faculty of  
Auburn University  
in partial fulfillment of the  
requirements for the Degree of  
Master of Science

Auburn, Alabama  
December 15, 2018

Keywords: *Pinus palustris* Mill., leaf water potential,  
sap flux density, throughfall exclusion, drought

Copyright 2018 by Michael Roldan Ramirez, Jr.

Approved by

Lisa Samuelson, Dwain G. Luce Professor of Forestry, Alumni Professor  
Art Chappelka, Professor of Forestry, Alumni Professor  
Amy Wright, Associate Dean for Instruction, Professor of Horticulture

## Abstract

Projections of increased frequency and severity of climatic- induced drought have raised concerns about the health, productivity and composition of forests in the southeastern United States. Longleaf pine (*Pinus palustris* Mill.) is a native species that thrives on sites that are frequently disturbed by fire and is thought to be more tolerant of drought stress than other southern pines, making it a suitable species to withstand future climate conditions. However, the limits and mechanisms of that presumed drought tolerance are not known. *In-situ* manipulation of water availability was used in this study to examine the effects of drought on water relations in a longleaf pine plantation. Specifically, the effects of a 40% reduction in throughfall precipitation on leaf water potential, sap flux density, whole-tree hydraulic conductance, and productivity were investigated. Following the installation of the throughfall reduction treatment in May 2016, a prolonged natural drought occurred wherein little to no precipitation fell on the site from September 2016 until the end of November 2016. Throughfall reduction did not influence leaf water potential or productivity during the 2016 natural drought but did reduce sap flux density and whole-tree hydraulic conductance. As natural drought conditions alleviated in 2017, the 40% throughfall reduction treatment did reduce sap flux density, but did not significantly affect leaf water potential, whole-tree hydraulic conductance, or productivity. Longleaf pine survived severe water deficit and throughfall reduction by reducing transpiration but not growth, and thus may be a suitable species for drought prone sites.

## Acknowledgments

This research would not have been possible without the considerable assistance from many people. First, I would like to thank my major advisor Dr. Lisa Samuelson for giving me the opportunity, support, and guidance to complete this project. I also appreciate the other members of my thesis committee, Dr. Art Chappelka and Dr. Amy Wright, for their guidance and advice. Next, I would like to thank Dr. George Matusick for his help getting the site established and coordinating with The Nature Conservancy. The Nature Conservancy also provided funding for the sap flow system. I would also like to thank Tom Stokes, Jake Blackstock, and John Lewis for introducing me to research and providing a bright side to digging taproots. I am also grateful to Stan Bartkowiak IV, Charles Pell, and Caren Mendonça not only for help with research and field work, but for the support I needed to figure out how to make it through graduate school. Of course, I would not be able to have done anything without the love and unwavering support of my parents, Mike and Kim Ramirez. I would also like to thank my sister for allowing me to vent and keep me grounded. I am also grateful to my grandparents Arnoldo Ramirez, Ted and Molly Jo Maki for being amazing examples of hard work and strong character. Finally, I would like to thank Sarah Wilson, for making it possible for me to get through this entire process through a bottomless amount of support.

## Table of Contents

<b>Abstract .....</b>	<b>ii</b>
<b>Acknowledgments.....</b>	<b>iii</b>
<b>Table of Contents.....</b>	<b>iv</b>
<b>List of Tables .....</b>	<b>vi</b>
<b>List of Figures .....</b>	<b>vii</b>
<b>List of Abbreviations .....</b>	<b>ix</b>
<b>1 Introduction .....</b>	<b>1</b>
1.1 Background.....	1
1.1.1 Longleaf Pine Ecosystem.....	1
1.1.2 Climate Change and Drought.....	3
1.1.3 Forest Response to Drought .....	4
1.1.4 Water Relations During Water Deficit.....	5
1.2 Objectives .....	11
<b>2 Impact of Drought and 40% Throughfall Reduction on Water Relations in a Longleaf Pine Stand.....</b>	<b>12</b>
2.1 Introduction .....	12
2.1.1 Objectives and Hypotheses .....	13
2.2 Materials and Methods.....	14
2.2.1 Site Description .....	14
2.2.2 Climate .....	16
2.2.3 Soil Moisture .....	18
2.2.4 Sap Flux Density .....	19
2.2.5 Leaf Water Potential and Whole-Tree Hydraulic Conductance.....	20
2.2.6 Leaf $\delta^{13}\text{C}$ and Specific Leaf Area .....	22
2.2.7 LAI and Growth.....	23
2.2.8 Statistical Analysis .....	24
2.3 Results .....	26
2.3.1 Climate .....	26
2.3.2 Soil Moisture .....	30

2.3.3	Water Potential .....	34
2.3.4	Sap Flux Density .....	39
2.3.5	Whole-Tree Hydraulic Conductance.....	41
2.3.6	Leaf $\delta^{13}\text{C}$ and Specific Leaf Area .....	45
2.3.7	LAI and Growth.....	46
2.4	Discussion.....	47
2.5	Conclusions .....	53
<b>3</b>	<b>References .....</b>	<b>56</b>

## List of Tables

Table 2.2.1. Pre-treatment characteristics of measurement plots (n=6) in an 11-year-old longleaf pine plantation. No pretreatment differences were detected.....	16
Table 2.2.2. Measurement frequency, start date, and end date of variables measured during the study. See Table 2.2.3 for specific leaf water potential ( $\Psi_L$ ) and leaf area index (LAI) measurement dates. ....	17
Table 2.2.3. Leaf water potential ( $\Psi_L$ ) and leaf area index (LAI) measurement dates. ....	22
Table 2.3.1. Mean (SE) foliar carbon-13 isotope composition ( $\delta^{13}C$ ), foliar nitrogen concentration (N), needle length, and specific leaf area (SLA) and observed probability values for two growing season flushes in response to throughfall treatment (TR; TR <sub>0</sub> , ambient throughfall; TR <sub>40</sub> , throughfall reduction) in a longleaf pine plantation in Marion County, Georgia measured in October 2016.....	45
Table 2.3.2. Mean (SE) basal area, density, DBH, height, and maximum leaf area index (LAI) in August in response to throughfall treatment (TR; TR <sub>0</sub> , ambient throughfall; TR <sub>40</sub> , throughfall reduction) and observed probability values in a longleaf pine plantation in Marion County, Georgia.....	46

## List of Figures

Figure 2.2.1. Research site location in Marion County, Georgia.....	14
Figure 2.2.2. Nested treatment and measurement plot design (A) and plot layout (B). .....	15
Figure 2.3.1. Daily (A) and monthly (B) total precipitation at the study site in Marion County, Georgia from June 2016 to September 2017. Thirty-year averages (1986-2017) of monthly summed precipitation were calculated using data from nearby Americus, Georgia. Source: NOAA National Centers for Environmental Information. <a href="http://www.ncdc.noaa.gov/cag/">http://www.ncdc.noaa.gov/cag/</a> .....	27
Figure 2.3.2. The Palmer Drought Severity Index (PDSI) for west central Georgia (Climate Division 4) from January 2016 to September 2017. Source: NOAA National Centers for Environmental Information. <a href="http://www.ncdc.noaa.gov/cag/">http://www.ncdc.noaa.gov/cag/</a> .....	28
Figure 2.3.3. Daily average vapor pressure deficit (D) at the study site in Marion County, Georgia from June 2016 to September 2017.....	28
Figure 2.3.4. Daily (A) and monthly (B) minimum ( $T_{\min}$ ), maximum ( $T_{\max}$ ), and mean temperatures at the study site in Marion County, Georgia from June 2016 through September 2017. ....	29
Figure 2.3.5. Mean daily soil moisture ( $\theta$ ) at 5 cm (A), 15 cm (B), 50 cm (C), and 100 cm (D) depths in response to throughfall treatment ( $TR_0$ , ambient throughfall; $TR_{40}$ , throughfall reduction) in a longleaf pine plantation in Marion County, Georgia measured from July 2016 to September 2017. ....	32
Figure 2.3.6. Mean daily soil moisture ( $\theta$ ) at 5 cm (A), 15 cm (B), 50 cm (C), and 100 cm (D) depths in response to throughfall treatment ( $TR_0$ , ambient throughfall; $TR_{40}$ , throughfall reduction) in a longleaf pine plantation in Marion County, Georgia measured from July 2016 to September 2017. Soil moisture in $TR_{40}$ has been scaled to plot-level.....	33
Figure 2.3.7. Mean ( $\pm$ SE) predawn ( $\Psi_{PD}$ ) and midday ( $\Psi_{MD}$ ) leaf water potential and the difference between the two ( $\Delta\Psi$ ) in response to throughfall treatment ( $TR_0$ , ambient throughfall; $TR_{40}$ , throughfall reduction) in a longleaf pine plantation in Marion	

County, Georgia measured from July 2016 to September 2017. Observed probability values for treatment and date effects are shown by year.....	35
Figure 2.3.8. Predawn leaf water potential ( $\Psi_{PD}$ ) response to soil moisture ( $\theta$ ) at 5 cm in a longleaf pine plantation in Marion County, Georgia measured from July 2016 to September 2017. ....	36
Figure 2.3.9. Midday leaf water potential ( $\Psi_{MD}$ ) response to plot-level soil moisture ( $\theta$ ) at 5 cm depth in a longleaf pine plantation in Marion County, Georgia measured from July 2016 to September 2017.....	37
Figure 2.3.10. Midday leaf water potential ( $\Psi_{MD}$ ) in response to predawn leaf water potential ( $\Psi_{PD}$ ) in a longleaf pine plantation in Marion County, Georgia measured from July 2016 to September 2017, but excluding data measured from October 2016 through December 2016. A 1:1 line is included for reference.....	38
Figure 2.3.11. Mean ( $\pm$ SE) sap flux density ( $J_v$ ) at midday in response to throughfall treatment ( $TR_0$ , ambient throughfall; $TR_{40}$ , throughfall reduction) in a longleaf pine plantation in Marion County, Georgia measured from July 2016 to September 2017.....	39
Figure 2.3.12. Mean ( $\pm$ SE) sum of daily sap flux density ( $J_\Sigma$ ) in response to throughfall treatment ( $TR_0$ , ambient throughfall; $TR_{40}$ , throughfall reduction) in a longleaf pine plantation in Marion County, Georgia measured from July 2016 to September 2017. * Indicates a significant throughfall treatment effect within a date.....	40
Figure 2.3.13. Mean ( $\pm$ SE) whole-tree hydraulic conductance ( $K$ ) in response to throughfall treatment ( $TR_0$ , ambient throughfall; $TR_{40}$ , throughfall reduction) in a longleaf pine plantation in Marion County, Georgia measured from July 2016 to September 2017. ....	41
Figure 2.3.14. Whole-tree hydraulic conductance ( $K$ ) response to predawn water potential ( $\Psi_{PD}$ ) in a longleaf pine plantation in Marion County, Georgia measured from July 2016 through November 2016. ....	43
Figure 2.3.15. Whole-tree hydraulic conductance ( $K$ ) response to midday water potential ( $\Psi_{MD}$ ) in a longleaf pine plantation in Marion County, Georgia measured from July 2016 through November 2016. ....	44



## List of Abbreviations

$^{12}\text{C}$	Carbon-12 isotope
$^{13}\text{C}$	Carbon-13 isotope
$A_{\text{SURF}}$	Needle surface area
BA	Basal area
C	Soil capacitance
$C_p$	Specific heat of air
D	Vapor pressure deficit
DBH	Diameter at breast height
$D_L$	Needle diameter
dT	Temperature difference
$dT_{\text{max}}$	Maximum temperature difference
F	Geometrical factor
ha	Hectare
J	Energy, joules
$J_v$	Sap flux density
$J_{\Sigma}$	Sap flux density, daily total
K	Whole-tree hydraulic conductance
$K_G$	Dimensionless flux index (Grainier 1985)

L	Needle length
LAI	Leaf Area Index
min	Minute
n	Number of needles in fascicle bundle
NSC	Nonstructural Carbon
$\rho$	Density of air
PDSI	Palmer Drought Severity Index
R	Resistance
R'	Relative water content
SLA	Specific Leaf Area
SLW	Specific Leaf Weight
TDP	Thermal Dissipation Probe
TR <sub>0</sub>	Ambient throughfall reduction treatment
TR <sub>40</sub>	40% throughfall reduction treatment
V	Voltage at time t
V <sub>f</sub>	Applied voltage
V <sub>i</sub>	Starting voltage
WUE	Water Use Efficiency
$\alpha$	Alpha level
$\delta^{13}\text{C}$	Molar abundance ratio of carbon-13 isotope
$\Delta\Psi$	Water potential gradient
$\epsilon$	Dielectric permittivity
$\epsilon_0$	Permittivity of free space
$\theta$	Soil volumetric water content

$\theta_0$	Ambient treatment soil volumetric water content
$\theta_{40}$	Throughfall reduction treatment soil volumetric water content
$\theta_5$	Soil volumetric water content at 5 cm
$\theta_{15}$	Soil volumetric water content at 15 cm
$\theta_{50}$	Soil volumetric water content at 50 cm
$\theta_{100}$	Soil volumetric water content at 100 cm
$\Psi_L$	Leaf water potential
$\Psi_{MD}$	Midday leaf water potential
$\Psi_{PD}$	Predawn leaf water potential
$\Psi_{SOIL}$	Soil water potential

# 1 Introduction

## 1.1 Background

### 1.1.1 Longleaf Pine Ecosystem

Longleaf pine (*Pinus palustris* Mill.) once covered approximately 37 million ha of the Southeast [the majority of which was predominantly longleaf pine (Frost, 2006)], today longleaf pine forests have been reduced to 1.2 million ha (Van Lear *et al.*, 2005). Industry, agriculture, predation, and changes to ecosystem drivers in longleaf pine's natural range contributed to the reduction (Frost, 2006). Commonly used for turpentine and timber production, the majority of virgin forests had been impacted by commercial operations by the 1920's (Frost, 2006). As human populations dispersed and increased across the region, wildfire was reduced to protect property. Fire is a critical component to the longleaf pine ecosystem, and its removal from the landscape significantly decreased longleaf pine populations (Jose *et al.*, 2006). Currently, longleaf pine stands make up 2% of the timberland in the southeastern United States (Oswalt *et al.*, 2012).

An open canopy and a fire-regulated understory characterize this species. Typical longleaf pine stand structure requires frequent fire to maintain low, savannah-like densities (Gilliam & Platt, 1999). Longleaf pine is intolerant of competition, so regular burning is important to reduce encroaching hardwoods and other pine species (Boyer, 1990). Fire aids longleaf pine regeneration, as longleaf pine seeds require bare soil to germinate (Boyer, 1990).

Burning decreases ground cover, increasing the odds dispersed longleaf pine seeds will fall to favorable sites. As a disturbance mediated ecosystem, the continued presence and dominance of adapted species depends on the recurrence of conditions that make the species' normal range inhospitable to competitors. Without regular fire, the longleaf pine ecosystem is successional to a mixed-hardwood species composition (Van Lear *et al.*, 2005).

Interest in longleaf pine restoration has been increased over the last two decades (Van Lear *et al.*, 2005; McIntyre *et al.*, 2018). As much as 352,000 ha of longleaf pine have been planted in the Coastal Plain subregion, which the species formerly dominated (Jose *et al.*, 2006), and is where most of current longleaf pine forested area (89%) occurs (Oswalt *et al.*, 2012). In 2007, a coalition of private and public groups developed America's Longleaf Restoration Initiative (ALRI), which set a goal to increase longleaf pine coverage by 1.5 million ha by 2025 (McIntyre *et al.*, 2018). The longleaf pine forest type increased by 85,500 ha between 2010 and 2015, although those gains have been offset by decreases of longleaf/oak forest type (McIntyre *et al.*, 2018). Further, the longleaf pine ecosystem is valued for its plant and animal biodiversity (Outcalt, 2000). From a management perspective, the longleaf pine savannah is most importantly facultative habitat for the endangered red-cockaded woodpecker (*Leuconotopicus borealis* Vieillot). Thus, habitat alteration restrictions included in the Endangered Species Act have aided longleaf pine conservation efforts.

While much of the restoration interest is ecological, longleaf pine stands can yield economic value. Longleaf pine grows with good form, as it is self-pruning and grows straight, yielding long, clear boles that are highly valuable as pole timber (Boyer, 1990; Outcalt, 2000). Longleaf pine needles are often used in landscaping applications, providing mid-rotation income to landowners (Outcalt, 2000). Game species are provided with good habitat due to

planting density and the open understory of a well-managed longleaf pine stand (Outcalt, 2000). Therefore, longleaf pine restoration is beneficial to many different interest groups.

### **1.1.2 Climate Change and Drought**

Increases in anthropogenic CO<sub>2</sub> since the Industrial Revolution have created alterations to climate patterns (IPCC, 2014). Through photosynthesis, southeastern forests remove CO<sub>2</sub> from the atmosphere and were estimated in 2010 to be a store of 12.4 billion tons of carbon (Wear & Gries, 2013). In the United States, carbon sequestration by forests offset an estimated 20% of carbon emitted between 2001 and 2005 (Lu *et al.*, 2015). The southeastern US is expected to lose between 4.5 million and 9.3 million ha (7% - 13%) of forested area to development over the next 40 years, with some sub-regions losing up to 21% (Wear & Gries, 2013). Planted pine is the only forest cover type that is expected to increase in area over the same time period. The forest industry contributed \$230.6 billion to the economic output of the Southeast in 2013 and supports about 1 million jobs (Boby *et al.*, 2014). Nationally, the SE is a leading source of softwood timber. In 2007, 60% of all timber produced in the US came from the SE (Wear & Gries, 2013). As an important component of the economy and carbon emission mitigation, therefore it is vital to understand the potential effects that projections of future climate may have on these forest ecosystems.

Mild droughts can be common in the Southeast during late summer (Hanson & Weltzin, 2000). Tree ring analysis shows that long term (~20 years) droughts have occurred in the past 1000 years (Seager *et al.*, 2009). Although drought is a natural part of forest ecosystems, climate change will alter the typical disturbance regimes (Dale *et al.*, 2001). Peak summer temperatures in the Southeast are expected to increase by 0.5-1.5° C over the next two decades (IPCC, 2013). Additionally, summer precipitation in the region has become increasingly variable as rain

events have become less frequent and more intense (Wang *et al.*, 2010). During the last thirty years, the percentage of summer days without rain has increased from approximately 35% to 45%, while the percentage of days of high rain events (where more than 10 mm of precipitation fell in a day) increased from ~12% to 18% (Wang *et al.*, 2010). Changes in summer precipitation patterns may have considerable impacts on natural systems as it alters water availability during growing season (Wehner, 2004; Li *et al.*, 2007). Alterations to precipitation patterns and increases in temperature may lead to increased drought frequency.

### **1.1.3 Forest Response to Drought**

Drought has been linked to tree mortality, and Allen *et al.* (2010) suggested that some forests may already be experiencing climate change related mortality events. In Texas in 2007, a 75% reduction of standard precipitation resulted in a severe year-long drought (Moore *et al.*, 2016). The widespread tree mortality that followed released substantial amounts of stored carbon, partially negating the mitigation value of the affected forests (Moore *et al.*, 2016). Trees that survive a drought may not recover to pre-disturbance levels of productivity, and therefore are increasingly vulnerable to mortality during subsequent droughts. For example, Berdanier & Clark (2015) reported that the majority of trees not able to return to pre-drought growth rates following a multiyear drought in North Carolina died during a subsequent drought a full ten years later.

The predicted rise in temperature will increase D, creating a greater evaporative demand on trees, which will further decrease available soil moisture (Will *et al.*, 2013). Vapor pressure deficit is a factor in stomatal closure and water usage, and thus important in understanding the response of trees to higher temperatures (McDowell *et al.*, 2013). Smaller trees may not survive low soil moisture, but larger trees with more established root systems may be less prone to

mortality (Dale *et al.*, 2001). Conversely, some literature suggests the crowns of larger trees (and the associated high water demand) make larger trees more susceptible to whole mortality than traditionally thought (Moore *et al.*, 2016).

The response of forests to climate change is the cumulative response of individuals to changes in their environment. If the individual can endure the changes it is considered “resistant” (Hodgson *et al.*, 2015). In plants, this is done by minimizing the damage the stress causes (Lambers *et al.*, 2008) or by limiting reductions in productivity (Mitchel 2016). If the plant species is not resistant but can avoid mortality, it has the potential to recover to pre-disturbance levels of productivity. The relative amount of time required to make that return is the “resilience” of that species (Mitchell *et al.*, 2016).

In light of the projected increase in temperatures over the coming decades, there has been interest in planting more drought-resistant species (Clark *et al.*, 2016). Tree ring chronologies show that longleaf pine growth more correlated with Palmer Drought Severity Index (PDSI) than temperature or precipitation alone, indicating that longleaf pine productivity is specifically impacted by drought and not just high temperatures or low precipitation (Henderson & Grissino-Mayer, 2009). However, like any tree species, longleaf pine is not completely immune to long-term water deficit effects. Drought can impact stomatal activity for as much as a year after the drought ends, altering carbon sequestration (Starr *et al.*, 2016).

#### **1.1.4 Water Relations During Water Deficit**

Leaf water potential is used as a measure of plant water status. As evapotranspiration occurs, water is moved from the soil through the hydraulic pathway of the tree and into the atmosphere through the stomata of the leaf (Lambers *et al.*, 2008). Water potential is by



convention a negative value, as it is hydrostatic pressure resulting from a suction tension rather than a positive pressure such as turgor (Lambers *et al.*, 2008). Therefore, in conventional terms,  $\Psi_L$  under well-watered conditions is “high” (i.e. negative, but relatively close to zero). When  $\theta$  is low, it is more difficult for water to move from the soil matrix into the root of the plant (Lambers *et al.*, 2008). Under the same amount of evaporative demand, the resultant  $\Psi_L$  would be less (more negative) than the  $\Psi_L$  under well-watered conditions. Water potential is a valuable measure not only used to assess water status, but to describe a plant species’ drought response and vulnerability to drought-induced mortality (McDowell *et al.*, 2008; Choat *et al.*, 2012; Klein, 2014; Steppe, 2018). Longleaf pine is commonly found on sandy or upland sites where water can be scarce, and it would therefore be expected that longleaf pine experiences low  $\Psi_L$ . However, in a study of mature (57-years-old on average) longleaf pine trees during drought in southwest Georgia,  $\Psi_L$  was as low as -0.8 MPa for predawn measurements and -1.7 MPa for midday measurements (Addington *et al.*, 2004).

By measuring water potential at its highest point ( $\Psi_{PD}$ ) and at its lowest point ( $\Psi_{MD}$ ), the gradient of xylem tension experienced by the tree during the day can be determined ( $\Delta\Psi = \Psi_{PD} - \Psi_{MD}$ ). The  $\Delta\Psi$  is useful for describing plant responses when soil water becomes less available (Meinzer *et al.*, 2014; Garcia-Forner *et al.*, 2015; Roman *et al.*, 2015). Across a season, Gonzalez-Benecke *et al.* (2011) reported a mean  $\Delta\Psi$  in longleaf pine of 0.94 MPa. We observed similar values of  $\Delta\Psi$ , except for the period at end of the drought in 2016 when  $\Delta\Psi$  declined sharply and subsequently recovered. The  $\Delta\Psi$  becomes important as soil moisture decreases and/or D increases. If  $\Delta\Psi$  becomes too large, the water within the plant’s xylem can embolize, creating air bubbles that block the xylem and limit water transport further up the tree (Brodribb & Hill, 2000). Embolisms and their effects can accumulate, appreciably decreasing

the tree's ability to transport water with repeated drought exposure (Gaylord *et al.*, 2015). Stomatal closure in response to low  $\Psi_L$  is a strategy to avoid hydraulic failure but closure decreases photosynthesis and carbon accumulation (Brodribb, 2003). Lower carbon intake may lead to “carbon starvation” or contribute to a tree's mortality by predation or disease, even in drought-adapted pine species (McDowell *et al.*, 2008; Berdanier & Clark, 2015; Gaylord *et al.*, 2015; Anderegg *et al.*, 2016).

The ability to move water from the soil and out through the leaves is very important to the survival of the tree, so  $J_v$ , the amount of flow through a given area over a given area of time, is used to assess water movement (Vandegehuchte & Steppe, 2013). As  $J_v$  is measured continuously, it can be used to understand changes in plant water use throughout various time scales (day, season, year, etc.). In longleaf pine on sandy soil in Georgia and Florida,  $J_v$  averaged  $1.9 \text{ mol m}^{-2} \text{ s}^{-1}$  at midday in trees ranging from 35 cm to 42 cm in diameter (Ford *et al.*, 2004; Gonzalez-Benecke *et al.*, 2011). Sap flux density is used with  $\Delta\Psi$  to calculate  $K$ , or the amount of water that flows through a given tree at a given time and xylem tension (Brodribb & Cochard, 2009). As embolisms accumulate, less water can flow, and  $K$  will be reduced. In temperate conifers, a 50% loss of the tree's intrinsic ability to move water (its hydraulic conductivity) can be lethal (Brodribb & Cochard, 2009; O'Brien *et al.*, 2017). Hydraulic conductance in longleaf pine has been estimated as approximately  $0.4 \text{ mol m}^{-2} \text{ s}^{-1} \text{ MPa}^{-1}$  when  $\theta$  at 50 cm depth was less than 10% (Addington *et al.*, 2004, 2006; Gonzalez-Benecke *et al.*, 2011).

Low  $\theta$  is a common result of prolonged drought. As  $\theta$  declines, soil water becomes more unavailable to trees as  $\Psi_{\text{SOIL}}$  decreases. Trees will adjust their stomatal behavior on a physiological level to cope with less available water in an attempt to survive the drought. Trees

have two water-use strategies to resist effects of water deficit: either shut down or maintain stomatal conductance. Shutting down conductance (isohydric response) limits water loss, but also limits photosynthesis and carbohydrate production, thereby increasing the risk of carbon starvation (McDowell *et al.*, 2008; Allen *et al.*, 2010). Isohydric plants demonstrate increased stomatal sensitivity to changes in D in order to maintain a tolerable tension in the water column (Sperry & Love, 2015). Stomatal sensitivity to D is common in *Pinus* species (Addington *et al.*, 2004; Domec *et al.*, 2009; Poyatos *et al.*, 2013). Stomatal closure can alter the role of forests as a carbon sink, turning them into a source of carbon through respiration, and diminishing their mitigating benefits to CO<sub>2</sub> emissions (Starr *et al.*, 2016). Lower stomatal conductance means less carbon assimilation, and possibly reductions in productivity. Additionally, isohydric species have been observed allocating more carbon to non-structural carbohydrates (such as soluble sugars and starches) in the roots than to growth (Kannenberg *et al.*, 2017). Carbohydrate stores in stems are also used to compensate for lower C assimilation in isohydric species (Kannenberg *et al.*, 2017).

There have been several different ways of describing isohydric/anisohydric behavior (Tardieu & Simonneau, 1998; Klein, 2014; Maritz-Vilalta *et al.*, 2014; Meinzer *et al.*, 2016; Hochberg *et al.*, 2017; Lavoie-Lamoureux *et al.*, 2017). A typical isohydric species response is to control stomata to strictly limit low xylem water potential to avoid embolism (Tardieu & Simonneau, 1998; McDowell *et al.*, 2008). Perfectly isohydric trees under drought will reduce stomatal conductance and decrease sensitivity to D as soil water potential declines (Roman *et al.*, 2015). Other definitions of isohydry also use leaf water responses to changes in available moisture in the environment. Definitions of isohydry include: the maintenance of constant  $\Psi_{MD}$  with decreasing  $\theta$  (Tardieu & Simonneau, 1998), relatively small  $\Delta\Psi$  (Klein, 2014), or

where the slope of  $\Psi_{MD}/\Psi_{PD} < 1$  (Maritnez-Vilalta *et al.*, 2014; Meinzer *et al.*, 2016). It is expected that reductions in stomatal conductance will occur to prevent dangerously low  $\Psi_L$ , and  $\Delta\Psi$  will decrease as soil water potential declines (Roman *et al.*, 2015). The risk accompanying isohydric strategy lies in carbon accumulation, as trees limit stomatal conductance and therefore photosynthesis and may face carbon starvation if the drought is prolonged (McDowell *et al.*, 2008). The anisohydric response to drought is typified by maintaining stomatal conductance and allowing  $\Delta\Psi$  to increase with declining  $\theta$  (McDowell *et al.*, 2008; Roman *et al.*, 2015). As with isohydry, there are numerous definitions of anisohydry. Anisohydric behavior has been defined as decreasing  $\Psi_{MD}$  with declining  $\Psi_{SOIL}$  (Tardieu & Simonneau, 1998), relatively large  $\Delta\Psi$  (Klein, 2014), and where the slope of  $\Psi_{MD}/\Psi_{PD} > 1$  (Maritnez-Vilalta *et al.*, 2014; Meinzer *et al.*, 2016). Stomata of anisohydric species are not particularly sensitive to changes in D (Franks *et al.*, 2007). The perfectly anisohydric tree would, under drought stress, risk hydraulic failure in the xylem for continued carbon accumulation (McDowell *et al.*, 2008).

It is important to state that most tree species do not fall neatly into one category or the other, but fall in a continuum of responses that individual species can express (Klein, 2014; Maritnez-Vilalta *et al.*, 2014; Martínez-Vilalta & Garcia-Forner, 2016). Additionally, the direct mechanisms of drought-related mortality are not known, and the paths to mortality suggested in McDowell *et al.* (2008) are not wholly accepted (Sala *et al.*, 2010). Other research puts the risks and rewards of each strategy into question. In studies of Western ecosystems under drought, stomatal conductance was not found to be different between classically isohydric and anisohydric species, indicating that neither would be more carbon limited during drought than the other (Garcia-Forner *et al.*, 2016a). The isohydric conifer species also showed more

evidence of embolism than the anisohydric species, despite tight control of  $\Psi_{MD}$ . Other comparisons have also shown little differences in growth rate between isohydric and anisohydric species during drought (Garcia-Forner *et al.*, 2016b). Others have suggested that stomatal regulation of  $\Psi_L$  cannot be used as an indicator of future drought mortality, as stomatal sensitivity is relative to the tensions an individual species is accustomed to experiencing (Martínez-Vilalta & Garcia-Forner, 2016). Furthermore, some have suggested abandoning the isohydric/anisohydric concept altogether in favor of examining maximum transpiration, maximum K, and  $\Psi_L$  at hydraulic failure (Hochberg *et al.*, 2017).

Tree species that employ a more isohydric strategy can be disadvantaged when exposed to recurring drought as lower carbon accumulation can make less able to recover when drought conditions have abated, and less competitive for belowground resources (Salazar-Tortosa *et al.*, 2018). While pines are commonly considered isohydric (Zweifel *et al.*, 2009), xeric pine species have been observed using less-conservative water use strategies than mesic pine species, and have had higher growth and less mortality during drought (Salazar-Tortosa *et al.*, 2018)

## 1.2 Objectives

The primary objective of this study was to investigate the effects of increased drought severity (as compared to ambient conditions) on longleaf pine water relations and longleaf pine resilience. Changes in leaf water potential ( $\Psi_L$ ), sap flux density ( $J_V$ ), and whole-tree hydraulic conductance ( $K$ ) will be monitored in response to environmental variables such as soil moisture ( $\theta$ ) and vapor pressure deficit ( $D$ ). Responses of  $\Psi_L$ ,  $J_V$ , and  $K$  to  $\theta$  and  $D$  will be used to better understand the physiological mechanisms that may allow longleaf pine to survive prolonged drought, as well as the potential limits of those mechanisms. This information is valuable to land managers making decisions on existing mature stands, as well as selecting species for establishing new plantations. A 40% throughfall precipitation reduction treatment was applied to an 11-year old longleaf pine plantation located on well-drained soil to simulate drought on a site at the extreme fringes of drought vulnerability.

## 2 Impact of Drought and 40% Throughfall Reduction on Water Relations in a Longleaf Pine Stand

### 2.1 Introduction

Climate change is expected to increase the frequency and severity of droughts in the southeastern United States over the next half century (Wang *et al.*, 2010). Additionally, air temperatures are expected to increase by 0.5-1.5° C over the next twenty years (IPCC, 2013). The increase in temperature will likely increase evaporative demand and increase hydraulic stress on trees in the region (Will *et al.*, 2013). Pine trees make up a large part of the forested cover in the SE, and are an economically important source of timber for the region (Wear & Gries, 2013; Boby *et al.*, 2014). Increased climatic stress can lead to large mortality events, so it is important to understand the potential physiological responses trees might exhibit to avoid mortality (Moore *et al.*, 2016). Longleaf pine (*Pinus palustris* Mill.) is a native southern pine species that is commonly found on sandy, well drained sites and is thought to be more tolerant of drought than other southern pine species. While several studies have compared productivity and leaf physiology on mesic and xeric sites (Sheffield *et al.*, 2003; Addington *et al.*, 2006; Wright *et al.*, 2013), a controlled study of drought effects on longleaf pine in the field has not been done. To investigate the effects of prolonged periods of decreased water availability on longleaf pine, a 40% throughfall reduction treatment was installed in an 11-year-old longleaf pine plantation in western Georgia. To evaluate the effect of prolonged drought

on longleaf pine water relations, we monitored leaf water potential ( $\Psi_L$ ), sap flux density ( $J_v$ ), and whole-tree hydraulic conductance ( $K$ ) for their response to vapor pressure deficit ( $D$ ) and soil moisture ( $\theta$ ).

### **2.1.1 Objectives and Hypotheses**

The overall objective of this research is to examine the effects of a 40% throughfall reduction on the recovery of longleaf pine leaf and whole-tree hydraulic parameters:  $\Psi_L$ ,  $J_v$ , and  $K$ . Hypotheses to be tested include: (1) a 40% throughfall reduction will decrease  $\theta$ , leading to a decrease in predawn leaf water potential ( $\Psi_{PD}$ ) and midday leaf water potential ( $\Psi_{MD}$ ), and the gradient between  $\Psi_{PD}$  and  $\Psi_{MD}$  ( $\Delta\Psi$ ) will be maintained through stomatal control of  $\Psi_{MD}$ , (2) the carbon limitation associated with an isohydric response to 40% throughfall reduction will decrease aboveground growth in longleaf pine, and (3) a 40% throughfall reduction will compound the effects of natural drought, leading to slower recovery of  $J_v$  and  $K$  following natural drought, thereby decreasing drought resilience. This study is part of a long-term study investigating longleaf pine growth and changes in climate.



## 2.2 Materials and Methods

### 2.2.1 Site Description

The study was established in an 11-year-old longleaf pine plantation in Marion County, Georgia (32.553° N, 84.476° W) owned by the Georgia Department of Natural Resources and managed by The Nature Conservancy (Figure 2.2.1). Planting was done in 2005, at an approximate spacing of 2.6 m x 2.6 m. Nature Conservancy employees performed a prescribed burn in January 2016. The site lies in the Sand Hills ecoregion, where soils are typically of the Entisol order (Griffith *et al.*, 2001). The study is located near the boundary between the Piedmont and eastern Coastal Plain subregions (Figure 2.2.1) (Wear & Gries, 2013). Soils are Lakeland Series (2-5% slopes), which are deep, sandy, and excessively drained Thermic, coated Quartzipsamments (Soil Survey Staff, 2016). Site elevation is 211 m.



Figure 2.2.1. Research site location in Marion County, Georgia.

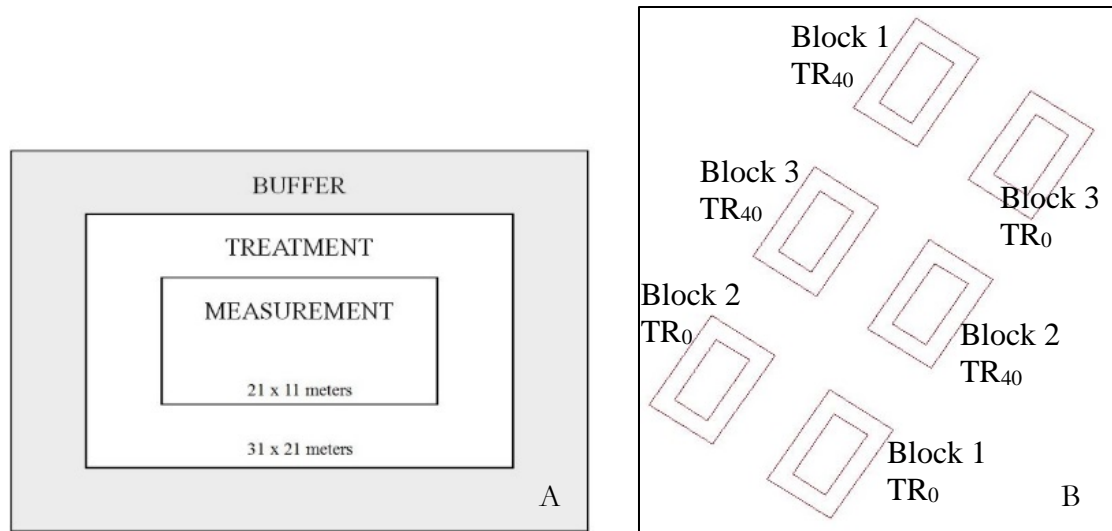


Figure 2.2.2. Nested treatment and measurement plot design (A) and plot layout (B).

The study design was a randomized complete block with two levels of throughfall treatment (TR): ambient throughfall (TR<sub>0</sub>) and an approximate 40% reduction of throughfall (TR<sub>40</sub>) replicated in three blocks. The 40% throughfall reduction represented the 1st quantile of annual precipitation for Americus, Georgia (32.065° N, 84.229° W; 60 km SE from site) over a 100-year period. The 0.07 ha treatment plots had approximately 17 m between plots (Figure 2.2.2). Approximately 70 trees were in each treatment plot. Intensively monitored measurement plots were located in the center 0.02 ha of each plot and encompassed about 25 trees. Blocks were based on similar pre-treatment basal area, which ranged from 17.0 to 20.4 m<sup>2</sup> ha<sup>-1</sup> (Table 2.2.1). The size of the 0.02 ha measurement plot was determined by excavating and measuring one root from three trees adjacent to the project site. Roots extended an average of 4.5 m from the base of the tree. By increasing the treatment 5m in all directions

around the measurement plot, trees were not likely able to access water from outside of the treated area.

Rain exclusion trays were installed between tree rows to cover approximately 40% of the total plot area in the TR<sub>40</sub> treatment. Trays were constructed at an average height of 1 m using 12-mil polyethylene sheeting (Polyscrim 12, Americover Inc., Escondido, California) and pressure treated lumber. Two 0.52 m wide exclusion troughs were built between tree rows, with a 0.48 m gap in-between to reduce soil-moisture banding. Sixteen troughs were installed per plot. Throughfall precipitation was intercepted by trays and collected in large corrugated pipes that carried water a minimum of 20 m off-plot.

Table 2.2.1. Pre-treatment characteristics of measurement plots (n=6) in an 11-year-old longleaf pine plantation. No pretreatment differences were detected.

Block	Treatment	BA (m <sup>2</sup> ha <sup>-1</sup> )	Density (stems ha <sup>-1</sup> )	Mean DBH (cm)	Mean Height (m)
1	TR <sub>0</sub>	20.4	1000	15.9	9.7
	TR <sub>40</sub>	19.8	1130	14.7	9.3
2	TR <sub>0</sub>	15.0	957	13.9	9.6
	TR <sub>40</sub>	17.0	1000	14.4	9.1
3	TR <sub>0</sub>	19.4	1130	14.5	9.6
	TR <sub>40</sub>	17.5	957	15.0	9.6

### 2.2.2 Climate

A weather station (6152 Vantage Pro 2 Wireless Weather Station, Davis Instruments, Vernon Hills, Illinois) was used to measure air temperature, wind-speed, and precipitation at thirty-minute intervals for the entirety of the study (Table 2.2.2). The station was set in a 0.65 ha clearing 500 m east of the project site, allowing unobstructed collection of precipitation data. Within the forest canopy, relative humidity and air temperature were measured approximately 2 m high at three locations in-between adjacent plots (HOBO U23 Pro v2

Temperature/Relative Humidity Logger, Onset Computer Corporation, Bourne, Massachusetts).

Table 2.2.2. Measurement frequency, start date, and end date of variables measured during the study. See Table 2.2.3 for specific leaf water potential ( $\Psi_L$ ) and leaf area index (LAI) measurement dates.

Variable	Frequency	Duration
Canopy Air Temperature	30 mins	April 2016 - September 2017
Canopy Relative Humidity	1 min, averaged and recorded 30 mins	September 2016 - September 2017
Climate	30 mins	April 2016 - September 2017
Growth	Annually	February 2016 - January 2018
LAI	3-4 weeks	February 2017 - September 2017
Precipitation	30 mins	April 2016 - September 2017
Sap Flow	1 min, averaged and recorded 30 mins	June 2016 - September 2017
Sapwood Area	Monthly	June 2016 – September 2017
Soil Moisture	1 min, averaged and recorded 30 mins	June 2016 - September 2017
Specific Leaf Area	Once	November 2016
Whole-Tree Hydraulic Conductance	3-4 weeks	July 2016 - September 2017
Wind Speed	30 mins	April 2016 - September 2017
$\delta^{13}\text{C}$	Once	November 2016
$\Psi_L$	3-4 weeks	June 2016 - September 2017

### 2.2.3 Soil Moisture

Soil volumetric water content ( $\theta$ ) was used to quantify the amount of water available to the study trees. We installed probes in every plot at three depths: 5 cm, 15 cm, and 50 cm. In every plot, probes were installed in the center of a row, near the center of the plot. Additionally, two plots in one block had a probe inserted at 100 cm. Probes in the treatment plots were placed under the rain exclusion trays to validate that throughfall reduction treatment was effective.

Soil volumetric water content was measured continuously and recorded every 30 minutes in all plots using 10 cm probes (10HS Large Soil Moisture Sensors, S-SMx-M005, Decagon Devices, Inc., Pullman, Washington) inserted at 5 cm, 15 cm, 50 cm, and 100 cm, and data loggers (HOBO Micro Logger Station Data Logger, Onset Computer Corporation, Bourne, Massachusetts). The probes generate an accumulating electromagnetic field in the soil and measure the time required to reach a particular charge ('10HS Soil Moisture Sensor Manual', 2016). That duration relates to the capacitance of the soil ( $C$ ) (Equation 1), which in turn relates to the dielectric permittivity ( $\epsilon$ ) of the soil between the two prongs of the sensor which is analogous to  $\theta$  (Equation 2) as follows:

$$t = RC \ln \left[ \frac{V - V_f}{V_i - V_f} \right]$$

Equation 1

where  $R$  = resistance,  $V$  = voltage at time  $t$ ,  $V_i$  = starting voltage and  $V_f$  = applied voltage and:

$$C = \epsilon_0 \epsilon F$$

Equation 2

where  $\epsilon_0$  is the permittivity of free space and  $F$  is a geometrical factor.

The soil moisture sensors that were placed under a throughfall reduction tray measured a drier  $\theta$  than what the entire plot would have experienced (only 40% of the plot area was covered by trays), and only represent a point measurement of soil moisture. Therefore, the actual  $\theta$  for the entire treatment plots was better represented by a weighted average of  $\theta$ . Daily plot averages of  $\theta$  were calculated in both  $TR_0$  and  $TR_{40}$ . Then, by block, a weighted average was made to represent plot-level water potential using ambient treatment volumetric water content ( $\theta_0$ ) and throughfall reduction volumetric water content ( $\theta_{40}$ ):

$$\text{plot - level } \theta = (0.6 \times \theta_0) + (0.4 \times \theta_{40})$$

Equation 3

#### **2.2.4 Sap Flux Density**

A Dynamax sap flow system with 30 mm thermal dissipation probes (TDP) (TDP-30, Dynamax, Inc., Houston, Texas) was used to determine tree sap flow in four or five trees per measurement plot (30 trees total) (FLGS-TDP Sap Velocity System Model XM1000, Dynamax, Inc., Houston, Texas). Thermal dissipation probes monitor temperature differences between a heated probe and a reference probe ( $dT$ ). Probes were installed into selected trees at DBH and reflecting wrap was placed around trees to prevent stem heating. Sap flow trees were selected using the quantiles of total method (giving more weight to larger trees), to accurately represent the range of tree basal area in the plot, making the eventual scaling up of the sap flow data more representative of the stand (Martin et al., 1997; Čermák et al., 2004). The quantile of totals method selects trees that represent a portion of a desired biometric parameter; here plot basal area was used.

As water in the xylem flows across the heated probe, heat is carried away from the area around the heated probe, and the difference in temperatures between the heated and reference probe is reduced (Lu *et al.*, 2004). A relatively large difference in temperature between the two probes indicates a low amount of transpiration. When transpiration is low or zero, the difference in temperatures is at its maximum, as there is no movement in the water column to carry heated water away from the heated probe. The heat from the heated probe will radiate outwards and warm the reference probe. At night, once the trees have refilled and water has stopped moving through the tree,  $dT$  should theoretically be at its maximum ( $dT_{max}$ ). However, this was often not the case. To correct instances where  $dT_{max}$  was not attained at night,  $dT_{max}$  was set by using Baseliner, an open-source software for processing sap flow data (Oishi *et al.*, 2016). To make the correction, a regression line was plotted across a graph of several days' worth of sap flow data. The Baseliner software uses user-defined  $dT_{max}$  thresholds to set points for the regression. Granier (1987) showed that  $dT$  and  $dT_{max}$  were related to a dimensionless parameter  $K_G$  (Equation 4) and that  $K_G$  could be used to calculate sap flux density ( $J_v$ ) (Equation 5).

$$K_G = \frac{dT_{max} - dT}{dT}$$

Equation 4

$$J_v = 119 \times 10^{-6} K_G^{1.231}$$

Equation 5

### **2.2.5 Leaf Water Potential and Whole-Tree Hydraulic Conductance**

Leaf water potential of sap flow trees was measured every three or four weeks from June 2016 until September 2017 (Table 2.2.3) using a 1505D Pressure Chamber Instrument

(PMS Instruments, Albany, Washington). We collected leaf predawn water potential samples before sunrise and transpiration began, when  $\Psi_{PD}$  should be in equilibrium with the water potential of the soil ( $\Psi_{SOIL}$ ). Midday leaf water potential samples were collected during the middle of the day (1100–1300 EST). Until February 2017, four samples from each one of the sap flow trees (24 trees total) were measured. To aid in sample collection, permanent scaffolding was installed in February 2017. After installation, five samples were collected from at least two sap flow trees per plot, with additional samples taken from a third tree when available (19 trees total). Samples were taken from the most recent mature flush of tufts from as high in the canopy as possible, approximately 8 m high.

Once removed from the tree, samples were placed in a sealable plastic bag containing a moist paper towel and put into a cooler until measured to ensure sample integrity (Boyer, 1995). For each measured tree, the difference between the two water potential measures ( $\Delta\Psi = \Psi_{PD} - \Psi_{MD}$ ) was used in conjunction with  $J_v$  ( $\text{mol m}^{-2} \text{s}^{-1}$ ) to calculate whole-tree hydraulic conductance,  $K$  ( $\text{mol m}^{-2} \text{s}^{-1} \text{MPa}^{-1}$ ):

$$K = \frac{J_v}{\Psi_{MD} - \Psi_{PD}}$$

Equation 6



Table 2.2.3. Leaf water potential ( $\Psi_L$ ) and leaf area index (LAI) measurement dates.

Measurement	Year	Dates
$\Psi_L$	2016	7/20, 8/15, 9/1/, 9/22, 10/13, 11/3, 11/22, 12/7
	2017	2/17, 3/28, 4/18, 5/9, 6/8, 6/28, 7/19, 8/16, 9/8
LAI	2017	2/10, 2/23, 3/27, 4/17, 5/8, 6/7, 6/27, 7/19, 8/16, 9/7

### 2.2.6 Leaf $\delta^{13}\text{C}$ and Specific Leaf Area

Leaf  $\delta^{13}\text{C}$  was measured on foliage of sap flow trees. Leaf  $^{13}\text{C}/^{12}\text{C}$  fractionation is the preferential selection of the lighter  $^{12}\text{C}$  isotope over  $^{13}\text{C}$  by Rubisco (Lambers *et al.*, 2008). Rubisco reacts more easily with  $^{12}\text{C}$  and will use it more readily than  $^{13}\text{C}$ . Rubisco reacts more easily with  $^{12}\text{C}$ , and will use it more readily than  $^{13}\text{C}$ . However, for isohydric plants, as stomatal closure increases during drought photosynthesis (A) decreases and carbon becomes less available. Consequently, less  $^{12}\text{C}$  is available and more  $^{13}\text{C}$  will have to be used, despite the lower reactivity with Rubisco and the relative amount of  $^{13}\text{C}$  fixed in the leaf increases. A higher proportion of  $^{13}\text{C}$  in the plant is therefore an indicator of drought stress. The ratio between  $^{13}\text{C}$  and  $^{12}\text{C}$  is referred to as the molar abundance ratio (R). The R of a foliage sample was compared the R of a fossil standard to calculate  $\delta^{13}\text{C}$ :

$$\delta^{13}\text{C} = \left( \frac{R_{\text{sample}}}{R_{\text{standard}}} - 1 \right) * 1000$$

Equation 7

In October 2016, foliage samples were collected from sunlit foliage in the upper canopy of all sap flow trees and stored on ice until dried at 70° C for 72 hours. Samples were

then finely ground and sent to The University of Arkansas Stable Isotope Laboratory (2016) for  $^{13}\text{C}/^{12}\text{C}$  fractionation analysis.

Length and diameter of five fascicle bundles per sap flow tree were also measured in October 2016. The same tufts that provided samples  $^{13}\text{C}/^{12}\text{C}$  fractionation analysis were used for length and diameters samples. Needle surface area was calculated using:

$$A_{SURF} = \sum_{i=1}^n L_i \left( D_L + \frac{\pi D_L}{n} \right)$$

Equation 8

where  $A_{SURF}$  = surface area,  $L$  = needle length,  $D_L$  = needle diameter, and  $n$  = number of needles in the fascicle (however, only fascicle bundles with three needles were used). Needles were dried in a  $70^\circ\text{C}$  oven for 72 hours, and then weighed. Specific leaf area (SLA) was calculated as the ratio of needle surface area to mass.

### **2.2.7 LAI and Growth**

Treatment effects on leaf area index (LAI) were measured at least once a month (

Table 2.2.2) (LAI-2200C Plant Canopy Analyzer, LI-COR Inc., Lincoln, Nebraska). The LAI-2200C works by comparing the amount of light available to the sensor head under the tree canopy to unobstructed light monitored by a second sensor in an opening (Welles & Cohen, 1996). Five circular optical sensors within each sensor lens detect a conical segment of light (angled  $7^\circ$ ,  $23^\circ$ ,  $38^\circ$ ,  $53^\circ$ , and  $68^\circ$  from the sensor, respectively) that (in the case of the sensor under the canopy) was partially obscured by vegetation.

Measurements in each plot were taken along three transects (approximately 5 m), each starting from the northern side (facing south) and moving diagonally from one row to the adjacent row, ending at nearby tree. Transects varied in length (as the distance from the northern side of the measurement plot to the ending tree in the adjacent row varied). Transect length was divided evenly into five LAI measurement points. In the event a measurement point occurred too close to the scaffolding, that data point was removed from further calculations.

The above-canopy light measurements were automatically collected every 15 seconds from a stationary sensor placed in an opening (the same 0.65 ha clearing 500 m east of the project site where climate data was collected). The sensor was set up far enough away from the tree line to ensure an accurate measurement of above-canopy light conditions. The below-canopy measurements were paired to the open sky measurements using FV2200 v2.0 Software provided by the manufacturer. The software removed data collected by the fifth ring (68°) sensor because it sampled light from parts of the canopy beyond the measurement plot.

We conducted pre-treatment inventory on all plots in the study in 2016. Height (m), crown width (m), and DBH (cm) were measured on every tree within the treatment plot (Table 2.2.1). Annual tree growth was measured to assess productivity and recovery. Height was measured using a laser hypsometer (TruPulse 200, Laser Technology Inc., Centennial, Colorado).

### **2.2.8 Statistical Analysis**

The study was a randomized, complete block design with one treatment (ambient throughfall versus 40% reduction throughfall) replicated in three blocks. Individual leaf water potential measurements ( $\Psi_{PD}$  and  $\Psi_{MD}$ ) were averaged by tree. Because the experimental unit

was the block, variables were averaged by plot across the four trees. Repeated measurements were dependent; therefore, to avoid pseudoreplication, treatment effects were tested using repeated measures ANOVA with block as the random effect (PROC MIXED, SAS Institute Inc., Cary, North Carolina). Covariance structure for each variable was determined by minimizing the Akaike Information Criterion (AIC). For non-repeated measurements, ANOVA was used to test for treatment effects (PROC GLM, SAS Institute Inc., Cary, North Carolina), and were considered significant at  $\alpha = 0.05$ . Relationships between hydraulic parameters and soil moisture and precipitation were examined using linear and nonlinear regression analysis.

## 2.3 Results

### 2.3.1 Climate

During 2016, the site experienced an extreme drought. Beginning September 11, there were 78 continuous days without appreciable rainfall, until rain returned at the end of November (Figure 2.3.1). Mild drought conditions ( $-1.00 \geq \text{PDSI} \geq -1.99$ ) were present in the region beginning in March and had increased to severe drought ( $-3.00 \geq \text{PDSI} \geq -3.99$ ) by August (Figure 2.3.2). Extreme drought conditions ( $\text{PDSI} \leq -4.00$ ) were present October through December 2016. Monthly sums of precipitation were low in September, October, and November, with the majority of rainfall occurring in a few large events rather than being spread evenly through multiple events throughout the respective months (Figure 2.3.3). Daily average D ranged from 0.03 KPa in December 2016 to 1.9 KPa in June 2016 (Figure 2.3.3). Total precipitation during the 2016 measurement period was 489.7 mm, and air temperatures ranged from 38.6 °C in June to -4.1 °C in December (Figure 2.3.4).

By January 2017, the extreme drought conditions decreased to moderate drought conditions (Figure 2.3.2). Drought intensified to severe drought in February, when monthly precipitation fell below the 30-year average. Severe drought persisted until May, when above-average precipitation occurred and PDSI increased to an incipient wet spell ( $0.50 \leq \text{PDSI} \leq 0.99$ ). By June, PDSI had elevated to slightly wet conditions ( $1.00 \leq \text{PDSI} \leq 1.99$ ). The PDSI continued to increase through the end of the measurement period, at which point conditions were moderately wet ( $2.00 \leq \text{PDSI} \leq 2.99$ ). Total precipitation during the 2017 measurement period was 1029.2 mm (Figure 2.3.1). Air temperatures during the study in 2017 ranged from 35.8 °C in July to -8.7 °C in January and averaged 20.0 °C (Figure 2.3.4). Daily average D during ranged from a low of 0.05 KPa in January to a high of 1.6 KPa in May (Figure 2.3.3).

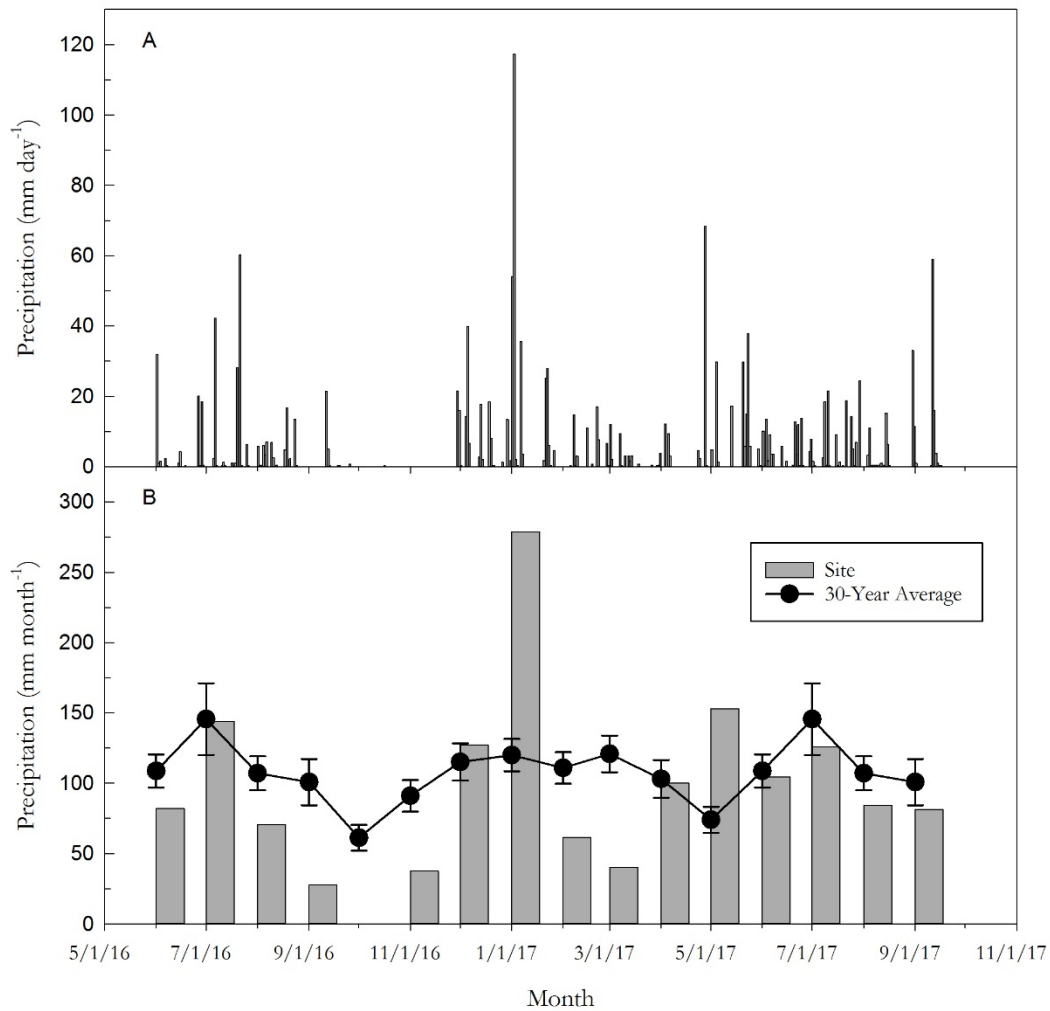


Figure 2.3.1. Daily (A) and monthly (B) total precipitation at the study site in Marion County, Georgia from June 2016 to September 2017. Thirty-year averages (1986-2017) of monthly summed precipitation were calculated using data from nearby Americus, Georgia. Source: NOAA National Centers for Environmental Information. <http://www.ncdc.noaa.gov/cag/>

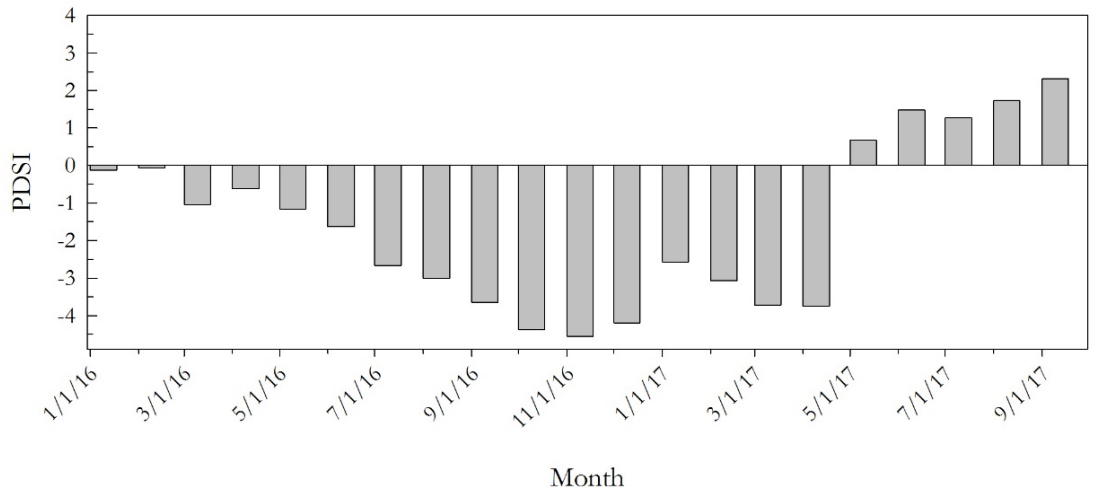


Figure 2.3.2. The Palmer Drought Severity Index (PDSI) for west central Georgia (Climate Division 4) from January 2016 to September 2017. Source: NOAA National Centers for Environmental Information. <http://www.ncdc.noaa.gov/cag/>

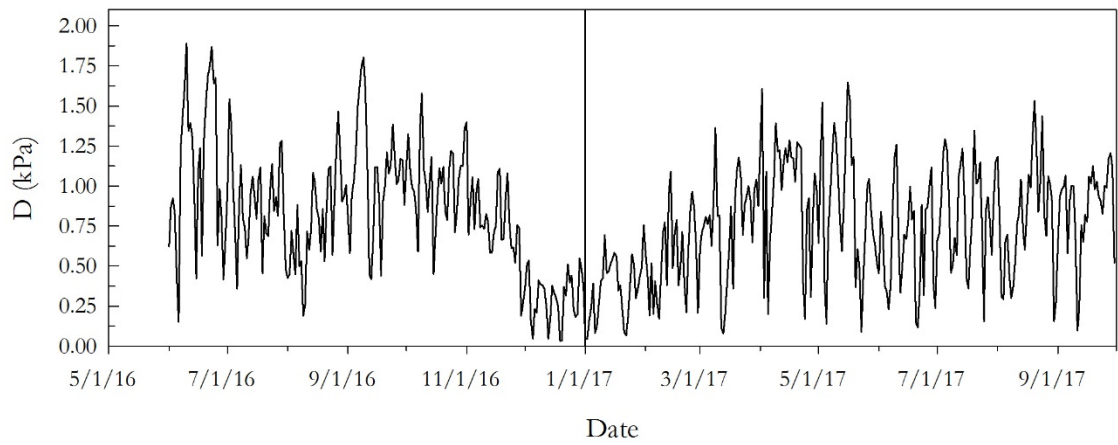


Figure 2.3.3. Daily average vapor pressure deficit (D) at the study site in Marion County, Georgia from June 2016 to September 2017.

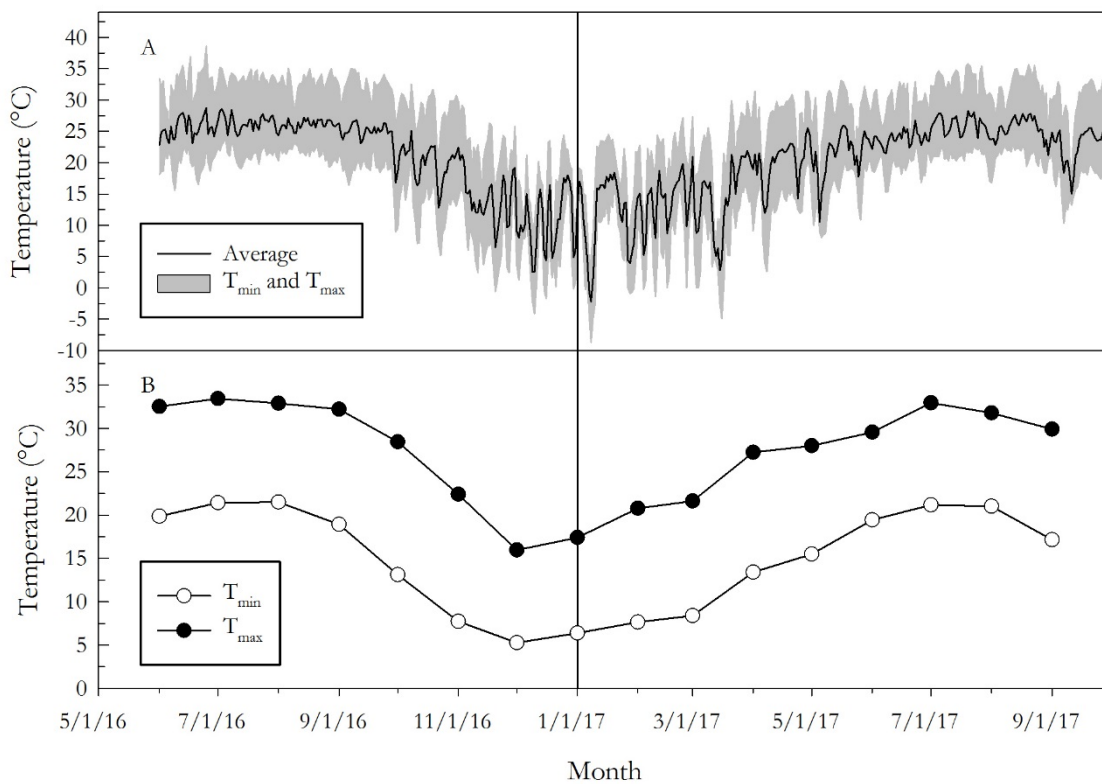


Figure 2.3.4. Daily (A) and monthly (B) minimum ( $T_{\min}$ ), maximum ( $T_{\max}$ ), and mean temperatures at the study site in Marion County, Georgia from June 2016 through September 2017.



### 2.3.2 Soil Moisture

The lack of precipitation in 2016 affected  $\theta$  in both treatments. Independent analysis of soil water-retention properties for soil at the site estimated the permanent wilting point at 3.1% (Tom Stokes, personal communication). In both treatments, point and plot-level  $\theta$  declined to  $<3\%$  during the drought at all depths (5 cm, 15 cm, 50 cm, and 100 cm), and remained low until precipitation resumed in late November (Figure 2.3.5, 2.3.6). Throughfall reduction trays reduced  $\theta$  directly under the trays (Figure 2.3.5) and were effective enough to decrease plot-level  $\theta$  (Figure 2.3.6). Plot-level  $\theta$  at 5 cm and 15 cm depths in TR<sub>40</sub> experienced extended periods below the permanent wilting point as early as 20 days before TR<sub>0</sub>, and declined to minimum drought-period soil moisture two days before TR<sub>0</sub> (Figure 2.3.6). At the 50 cm depth, plot-level  $\theta$  in TR<sub>0</sub> declined to the permanent wilting point two days before TR<sub>40</sub>. It took longer for plot-level  $\theta$  at 50 cm to recover from the period without precipitation than  $\theta$  at shallower depths. Volumetric soil moisture at 5 cm and 15 cm depths exceeded the permanent wilting point the same day as the first rain on November 28. At 50 cm, plot-level  $\theta$  increased past the permanent wilting point on December 4 in TR<sub>0</sub> and December 5 in TR<sub>40</sub>.

Across all blocks, average plot-level  $\theta$  in TR<sub>0</sub> during the 2016 measurement period was 4.6%, 4.1%, and 2.8% for 5 cm, 15 cm, and 50 cm depths, respectively (Figure 2.3.6). In TR<sub>40</sub> in the 2016 measurement, plot-level  $\theta$  averaged 4.1%, 3.7%, and 2.8% at 5 cm, 15 cm, and 50 cm depths respectively (Figure 2.3.6). During the 2017 measurement period, plot-level  $\theta$  at 5 cm, 15 cm, and 50 cm averaged 7.2%, 6.8%, and 4.3%, respectively, in TR<sub>0</sub> and 5.9%, 5.7%, and 4.1%, respectively, in TR<sub>40</sub>.

Point  $\theta$  (under the trays in TR<sub>40</sub> plots) also indicate an effect of throughfall reduction on  $\theta$  once precipitation resumed in November 2016. At 5 cm and 15 cm depths, TR<sub>40</sub> soils were

slower to show increases in point  $\theta$  and usually did not reach as high of  $\theta$  as soils in TR<sub>0</sub> (Figure 2.3.5). When  $\theta$  in TR<sub>40</sub> was scaled to the entire plot, differences are less pronounced but were still present (Figure 2.3.6). Often peaks in point  $\theta$  following precipitation events were higher in TR<sub>0</sub> plots than in TR<sub>40</sub>. This was especially true at 15 cm in 2016, where point  $\theta$  had a range of 10.3% in TR<sub>0</sub> plots but only 7.7% in TR<sub>40</sub> plots.

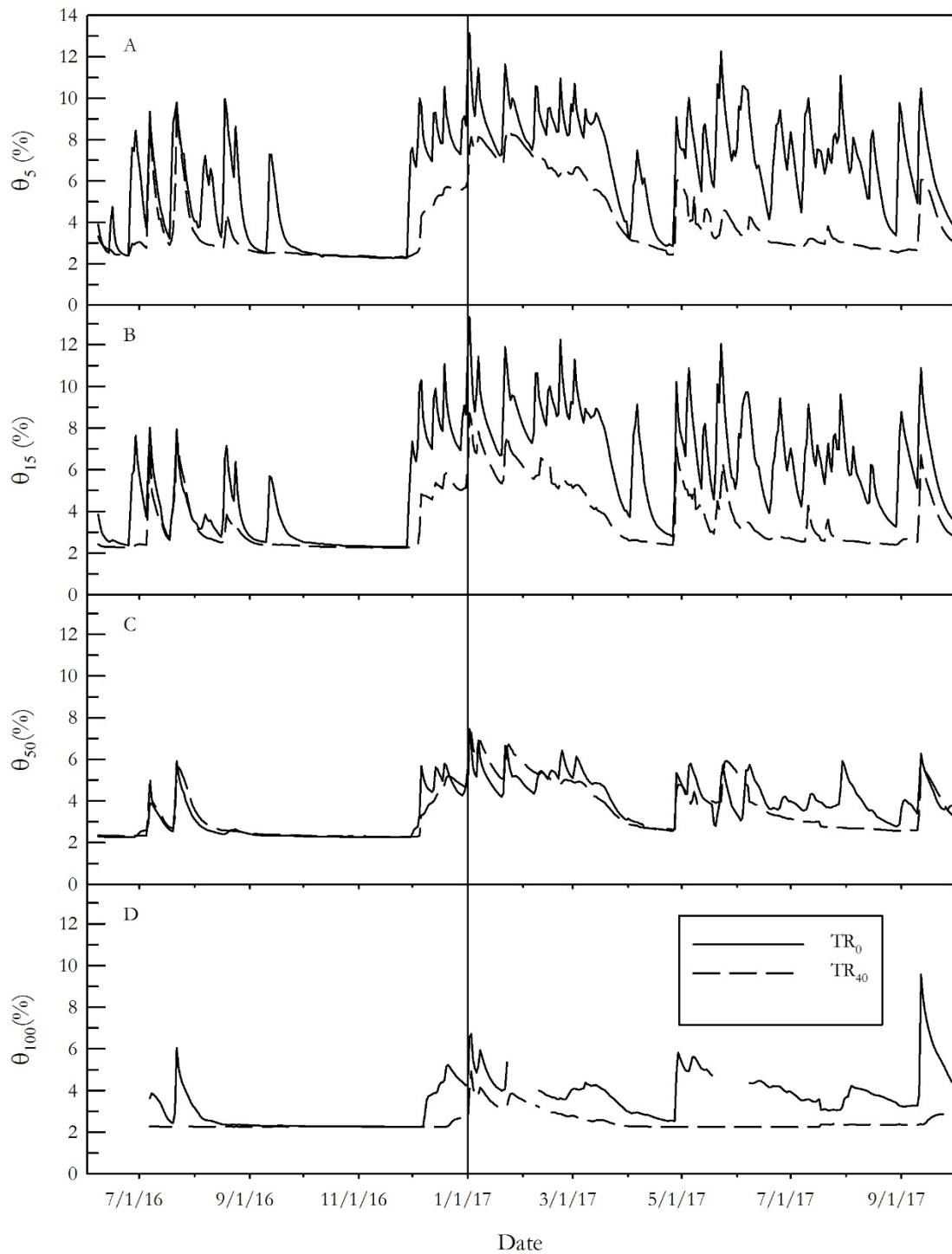


Figure 2.3.5. Mean daily soil moisture ( $\theta$ ) at 5 cm (A), 15 cm (B), 50 cm (C), and 100 cm (D) depths in response to throughfall treatment ( $TR_0$ , ambient throughfall;  $TR_{40}$ , throughfall reduction) in a longleaf pine plantation in Marion County, Georgia measured from July 2016 to September 2017.

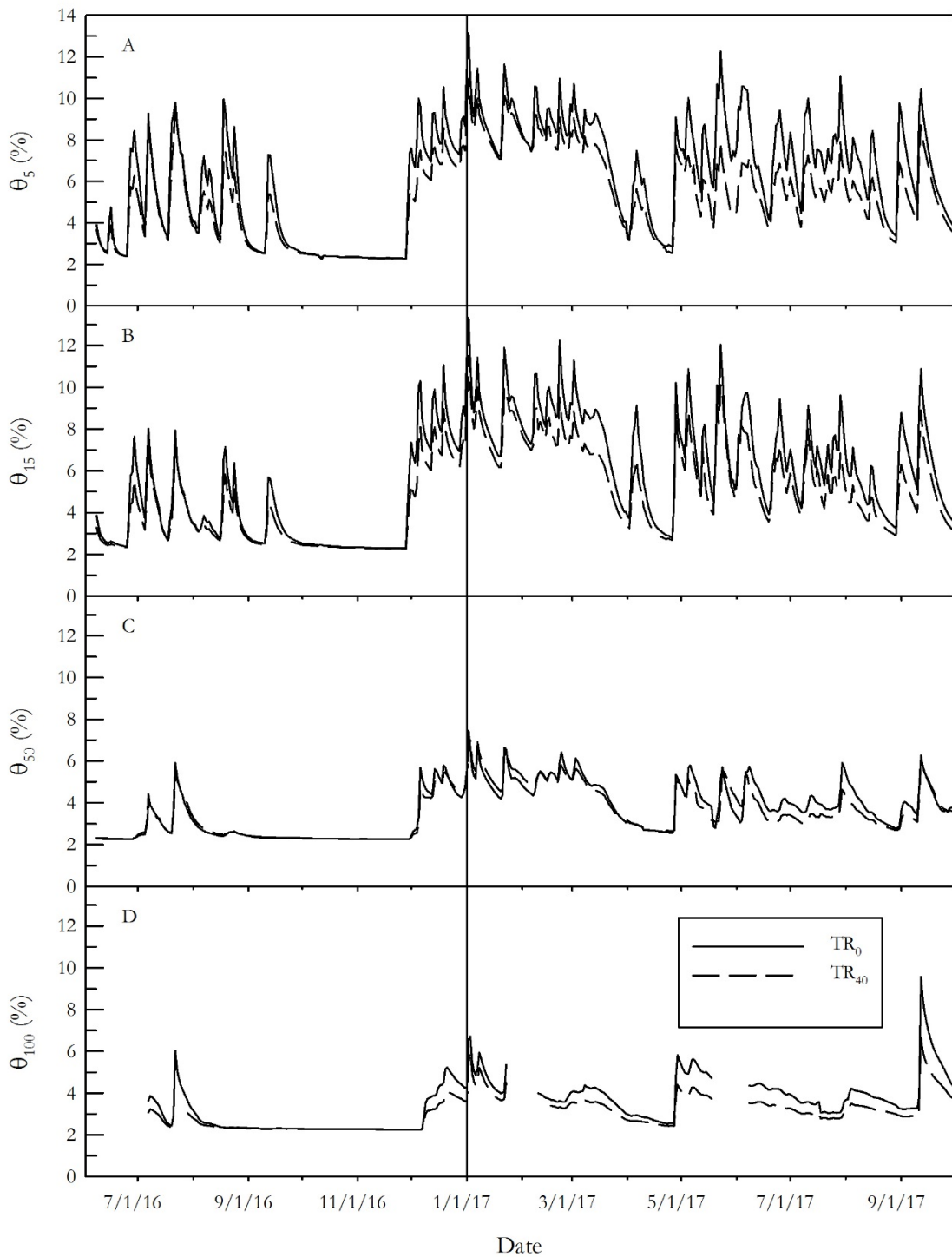


Figure 2.3.6. Mean daily soil moisture ( $\theta$ ) at 5 cm (A), 15 cm (B), 50 cm (C), and 100 cm (D) depths in response to throughfall treatment ( $TR_0$ , ambient throughfall;  $TR_{40}$ , throughfall reduction) in a longleaf pine plantation in Marion County, Georgia measured from July 2016 to September 2017. Soil moisture in  $TR_{40}$  has been scaled to plot-level.

### 2.3.3 Water Potential

No significant treatment differences or treatment by date interactions were detected for  $\Psi_{PD}$ ,  $\Psi_{MD}$ , and  $\Delta\Psi$  in 2016 and 2017 (Figure 2.3.7). In 2016 during the drought, predawn water potential declined in response to lack of precipitation and reduced soil moisture. The highest average  $\Psi_{PD}$  of 2016 was -0.8 MPa, and average  $\Psi_{PD}$  eventually declined to as low as -3.2 MPa during the drought. Minimum  $\Psi_{PD}$  in 2016 was much lower than the minimum  $\Psi_{PD}$  in 2017, which was -1.3 MPa. Midday water potential followed the same pattern as  $\Psi_{PD}$ , declining in 2016 from a high of -1.6 MPa to a low of -4.1 MPa as the drought persisted. Minimum  $\Psi_{MD}$  was markedly higher in 2017 (-2.1 MPa), however the maximum  $\Psi_{MD}$  was comparable (-1.4 MPa). The  $\Delta\Psi$  ranged from 0.0 MPa (when  $J_v$  was near-zero) to 1.5 MPa in 2016. In 2017,  $\Delta\Psi$  was as low as 0.2 MPa (when trees were returning to normal water potential gradients early in the year) and as high as 1.3 MPa.

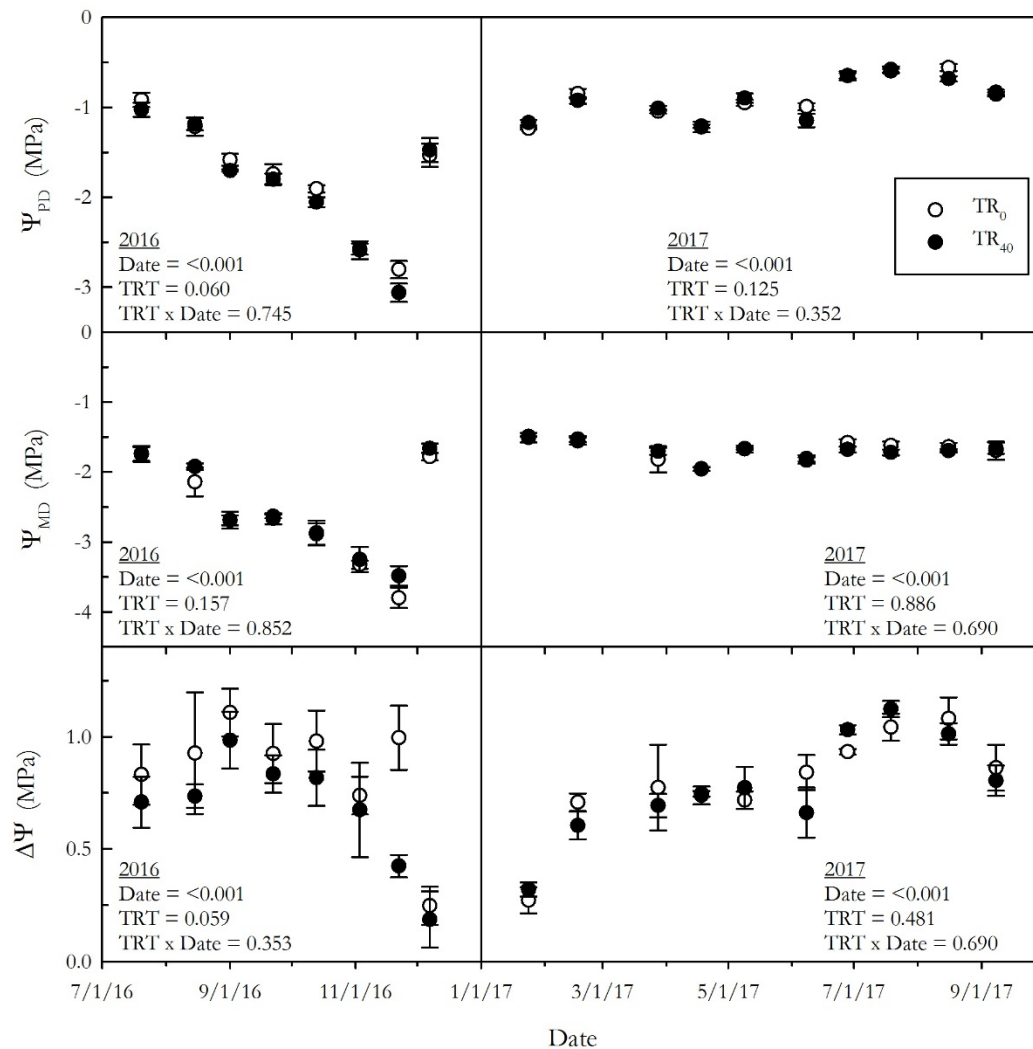


Figure 2.3.7. Mean ( $\pm$  SE) predawn ( $\Psi_{PD}$ ) and midday ( $\Psi_{MD}$ ) leaf water potential and the difference between the two ( $\Delta\Psi$ ) in response to throughfall treatment ( $TR_0$ , ambient throughfall;  $TR_{40}$ , throughfall reduction) in a longleaf pine plantation in Marion County, Georgia measured from July 2016 to September 2017. Observed probability values for treatment and date effects are shown by year.

Relationships between abiotic variables and  $\Psi_L$  were examined, and variation in  $\Psi_{PD}$  was best explained by soil moisture at 5 cm depth ( $\theta_5$ ) using a saturation curve ( $y = B_1x/(x + B_2)$ ), with 71% of the variation in  $\Psi_{PD}$  explained by  $\theta_5$  (Figure 2.3.8). Tests of the model coefficients fit by plot indicated that throughfall reduction did not affect the response of  $\Psi_{PD}$  to  $\theta_5$  ( $B_1, P = 0.423$ ;  $B_2, P = 0.423$ ). Predawn water potential was unresponsive to declining  $\theta_5$  until  $\theta_5$  reached 2.7%, at which point  $\Psi_{PD}$  and  $\theta_5$  became positively related.

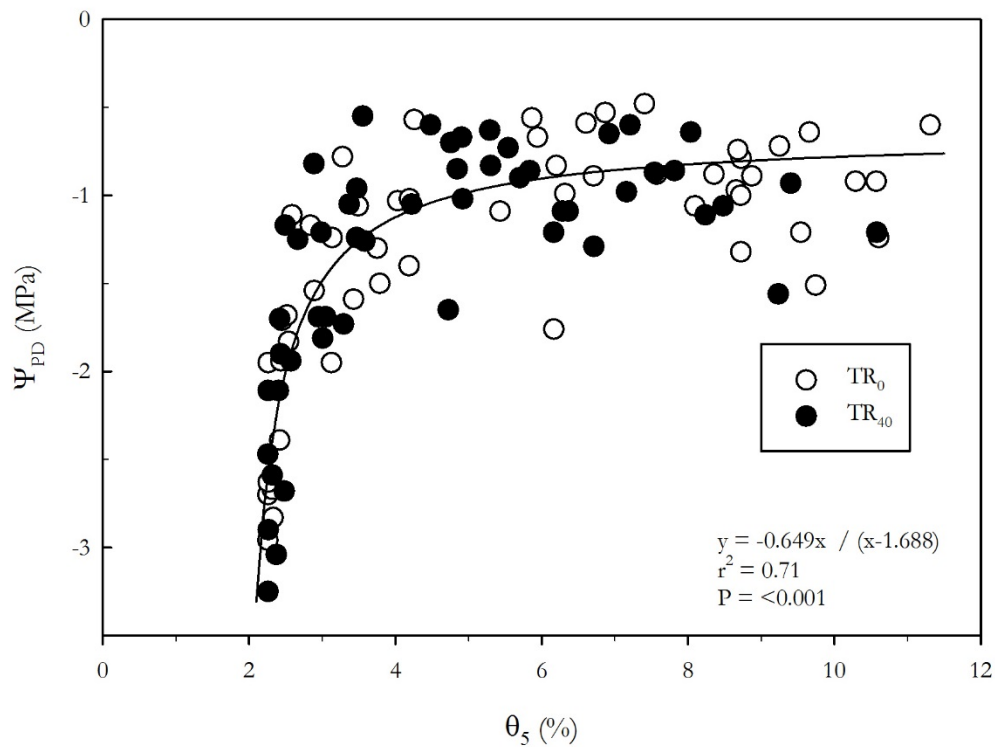


Figure 2.3.8. Predawn leaf water potential ( $\Psi_{PD}$ ) response to soil moisture ( $\theta$ ) at 5 cm in a longleaf pine plantation in Marion County, Georgia measured from July 2016 to September 2017.

Midday leaf water potential was also related ( $r^2=0.63$ ) to  $\theta_5$  (Figure 2.3.9). A power function ( $y = B_1(x^{B_2})$ ), rather than a saturation curve, provided the best fit. No treatment differences in the  $B_1$  ( $P = 0.089$ ) or  $B_2$  ( $P = 0.077$ ) coefficients were detected. Midday water potential was unresponsive to  $\theta_5$  until  $\theta_5$  declined to  $<4\%$ , then  $\Psi_{MD}$  declined rapidly.

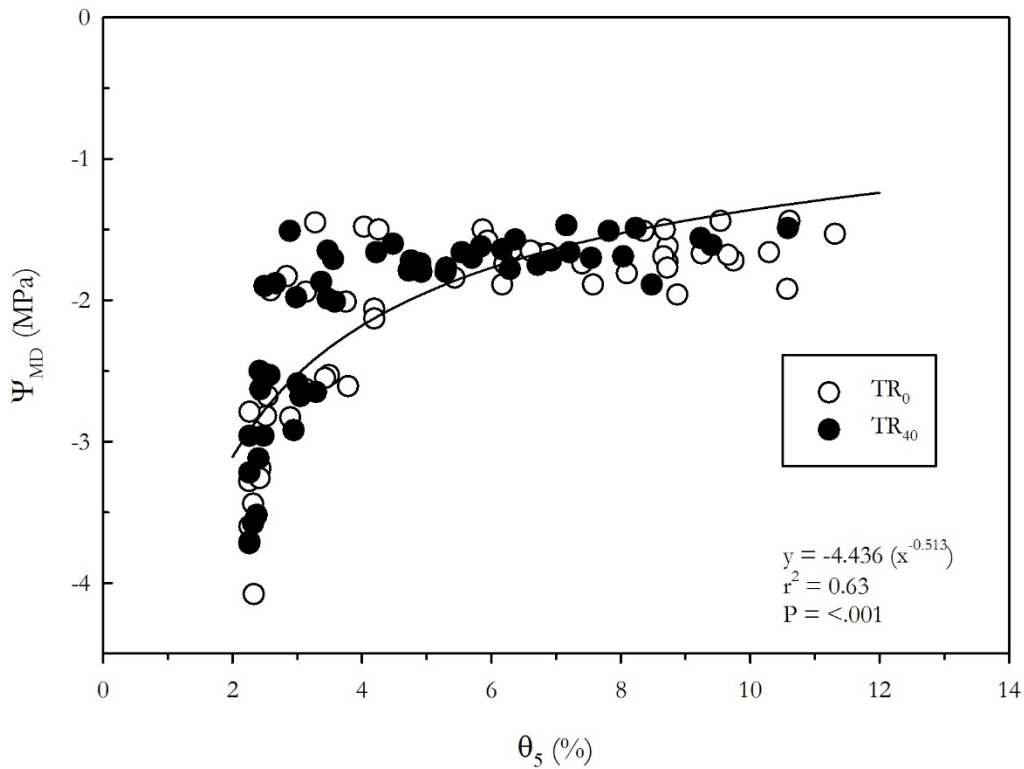


Figure 2.3.9. Midday leaf water potential ( $\Psi_{MD}$ ) response to plot-level soil moisture ( $\theta$ ) at 5 cm depth in a longleaf pine plantation in Marion County, Georgia measured from July 2016 to September 2017.



The relationship between  $\Psi_{PD}$  and  $\Psi_{MD}$  was also examined (Figure 2.3.10). Data from November 2016 through December 2016 were not included, as  $\Psi_L$  on those measurement dates were not regulated by stomatal control ( $J_v$  was near zero). A linear regression ( $y = B_0 + B_1x$ ) was fit to the data. No treatment differences were found for  $B_0$  ( $P = 0.824$ ) or for  $B_1$  ( $P = 0.827$ ). The slope of the relationship was 0.85.

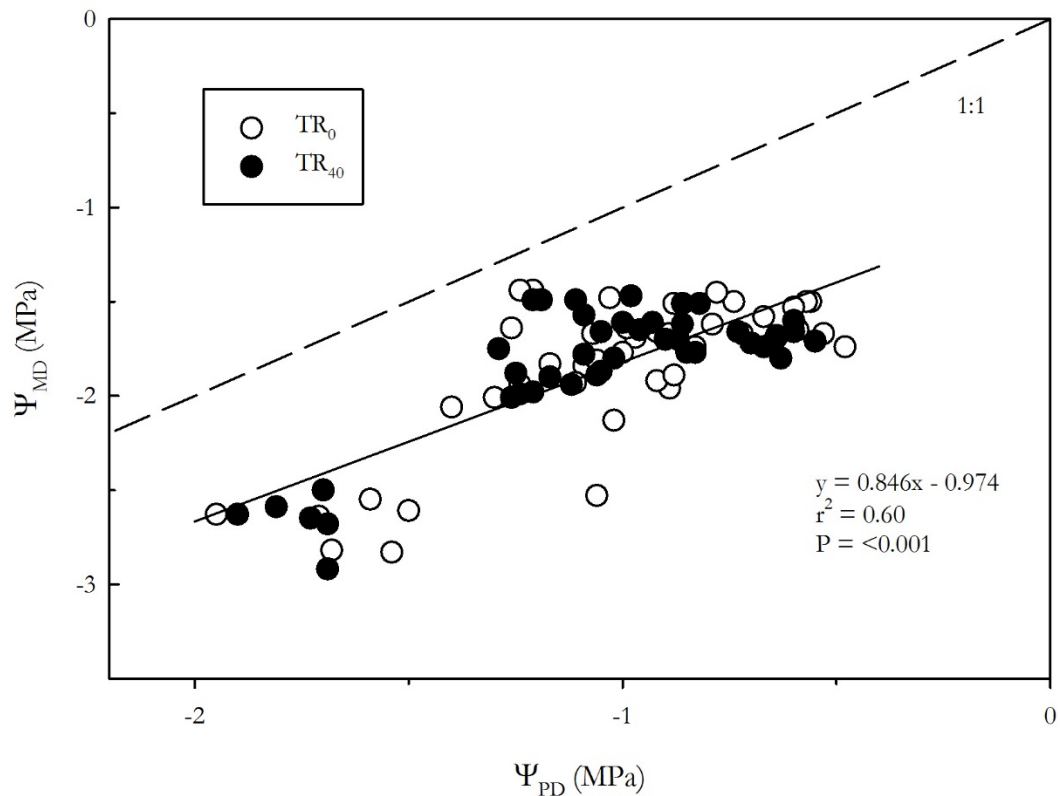


Figure 2.3.10. Midday leaf water potential ( $\Psi_{MD}$ ) in response to predawn leaf water potential ( $\Psi_{PD}$ ) in a longleaf pine plantation in Marion County, Georgia measured from July 2016 to September 2017, but excluding data measured from October 2016 through December 2016. A 1:1 line is included for reference.

### 2.3.4 Sap Flux Density

In 2016, the prolonged natural drought reduced  $J_v$ . Both midday and daily summed  $J_v$  declined as the drought progressed, decreasing to near-zero values in the last three measurements of the year (Figure 2.3.11, 2.3.12). Significant treatment differences in midday  $J_v$  were detected in 2016 as well as 2017. No significant treatment by date interactions were detected for midday  $J_v$  in 2016 or 2017. Throughfall reduction reduced midday  $J_v$  by 40% (from  $0.9 \text{ mol m}^{-2} \text{ s}^{-1}$  to  $0.6 \text{ mol m}^{-2} \text{ s}^{-1}$ ) in 2016 and by 14% (from  $2.1 \text{ mol m}^{-2} \text{ s}^{-1}$  to  $1.8 \text{ mol m}^{-2} \text{ s}^{-1}$ ) in 2017.

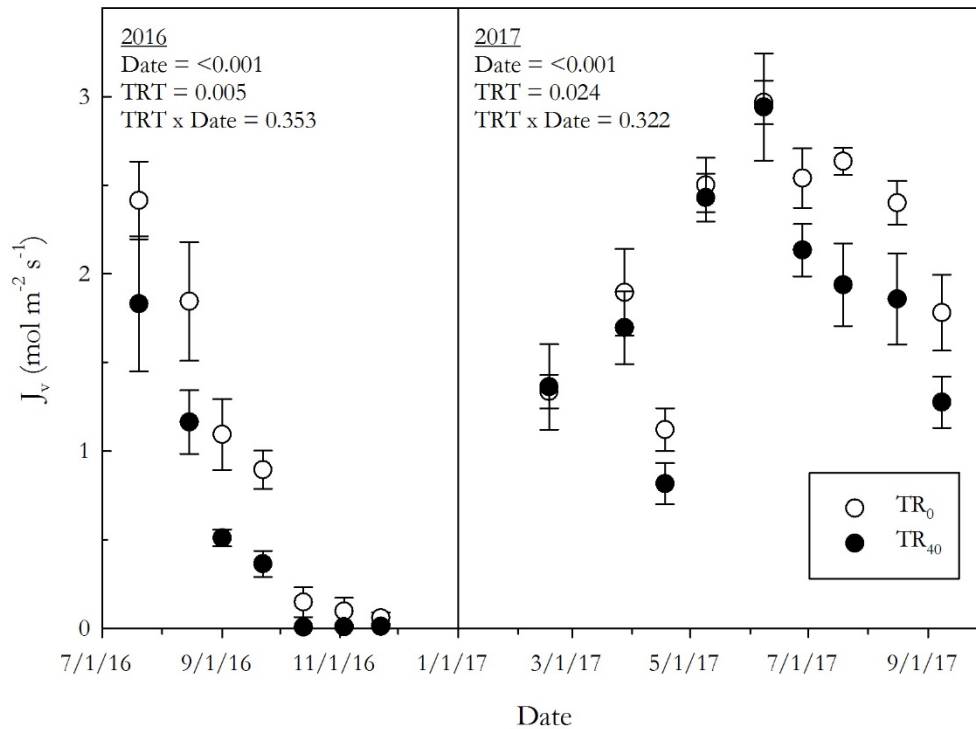


Figure 2.3.11. Mean ( $\pm$  SE) sap flux density ( $J_v$ ) at midday in response to throughfall treatment ( $\text{TR}_0$ , ambient throughfall;  $\text{TR}_{40}$ , throughfall reduction) in a longleaf pine plantation in Marion County, Georgia measured from July 2016 to September 2017.

In 2016, the daily sum of  $J_v$  ( $J_\Sigma$ ) ranged from 0.1  $\text{kg m}^{-2} \text{day}^{-1}$  on October 13 to 1612.2  $\text{kg m}^{-2} \text{day}^{-1}$  on July 20 (Figure 2.3.12). In 2017,  $J_\Sigma$  ranged from 338.0  $\text{kg m}^{-2} \text{day}^{-1}$  April 18 to 1919.4  $\text{kg m}^{-2} \text{day}^{-1}$  on June 8. We detected a significant interaction between treatment and date for  $J_\Sigma$  in both 2016, and 2017. In 2016,  $\text{TR}_{40}$  reduced  $J_\Sigma$  on July 20, August 15, and September 22 from 23.6% to 70.9%. In 2017,  $\text{TR}_{40}$  reduced  $J_\Sigma$  on July 19, August 16, and September 8 from 22.7% to 34.4%.

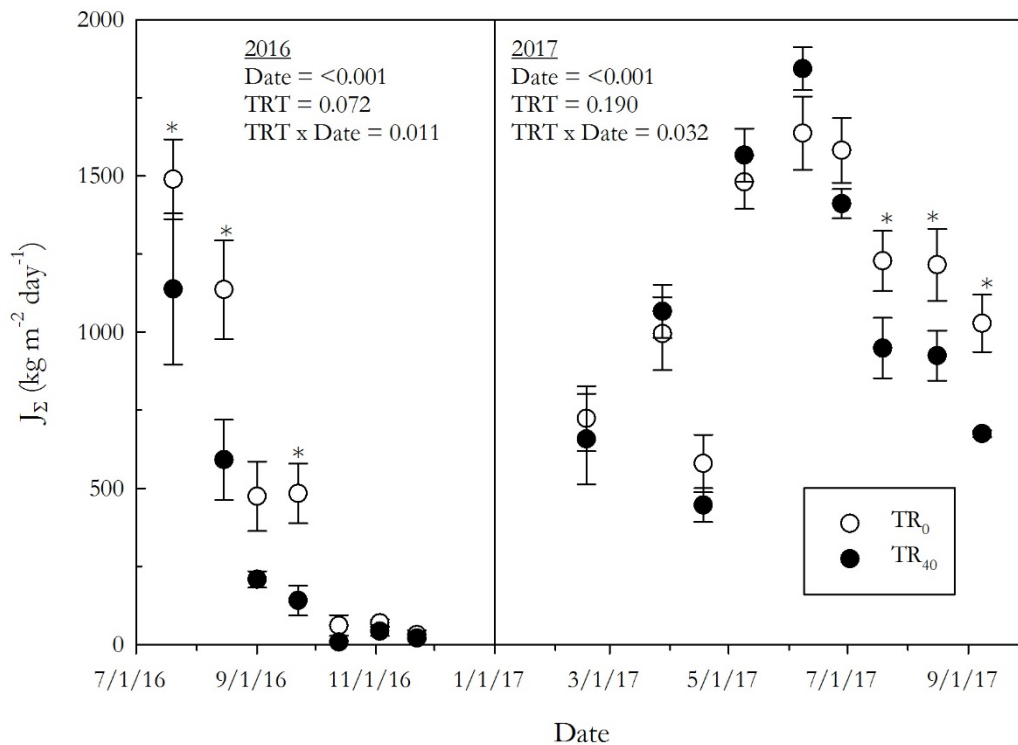


Figure 2.3.12. Mean ( $\pm$  SE) sum of daily sap flux density ( $J_\Sigma$ ) in response to throughfall treatment ( $\text{TR}_0$ , ambient throughfall;  $\text{TR}_{40}$ , throughfall reduction) in a longleaf pine plantation in Marion County, Georgia measured from July 2016 to September 2017. \* Indicates a significant throughfall treatment effect within a date.

### 2.3.5 Whole-Tree Hydraulic Conductance

In 2016, whole-tree hydraulic conductance declined during the drought, and was significantly different between treatments (Figure 2.3.13). In 2016, K in TR<sub>0</sub> was as low as 0.0 mol m<sup>-2</sup> s<sup>-1</sup> MPa<sup>-1</sup> and as high as 2.7 mol m<sup>-2</sup> s<sup>-1</sup> MPa<sup>-1</sup> and was on average 1.0 mol m<sup>-2</sup> s<sup>-1</sup> MPa<sup>-1</sup>. Throughfall reduction lowered K on average by 30.7% in 2016. In TR<sub>40</sub>, K ranged from 0.0 mol m<sup>-2</sup> s<sup>-1</sup> MPa<sup>-1</sup> to 2.5 mol m<sup>-2</sup> s<sup>-1</sup> MPa<sup>-1</sup> and averaged 0.7 mol m<sup>-2</sup> s<sup>-1</sup> MPa<sup>-1</sup>.

Whole-tree hydraulic conductance was not significantly different in 2017 (P = 0.570). In 2017, K ranged from 1.0 mol m<sup>-2</sup> s<sup>-1</sup> MPa<sup>-1</sup> to 5.6 mol m<sup>-2</sup> s<sup>-1</sup> MPa<sup>-1</sup> and averaged 2.4 mol m<sup>-2</sup> s<sup>-1</sup> MPa<sup>-1</sup>.

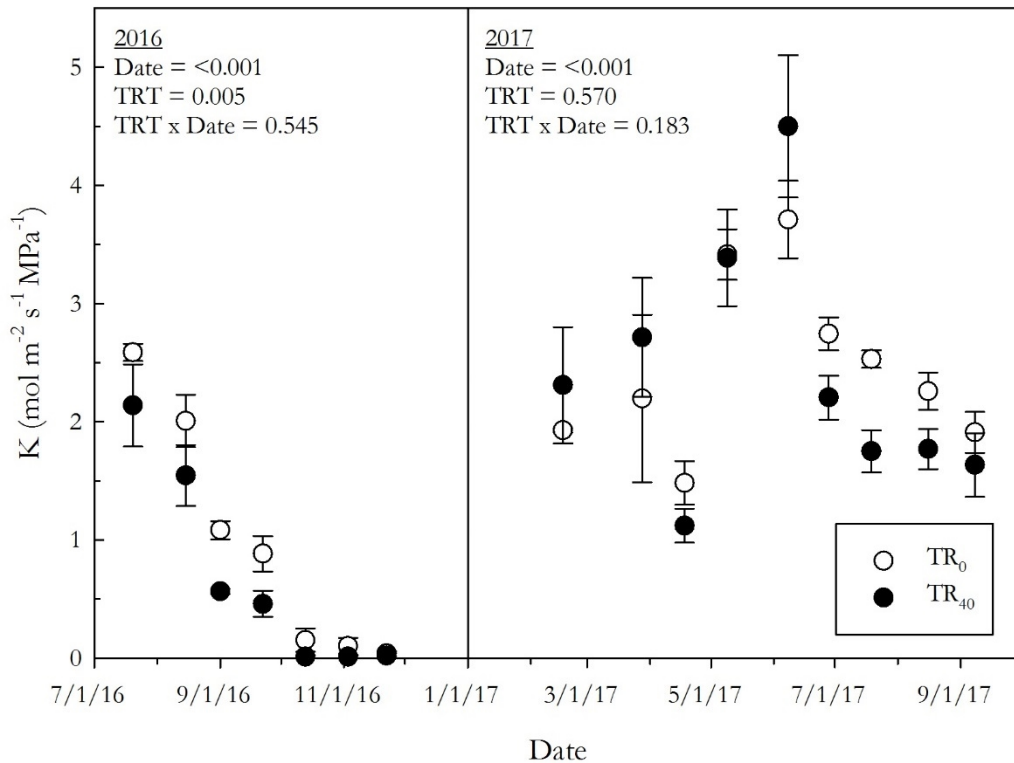


Figure 2.3.13. Mean ( $\pm$  SE) whole-tree hydraulic conductance (K) in response to throughfall treatment (TR<sub>0</sub>, ambient throughfall; TR<sub>40</sub>, throughfall reduction) in a longleaf pine plantation in Marion County, Georgia measured from July 2016 to September 2017.

The response of whole-tree hydraulic to changes in  $\Psi_{PD}$  and  $\Psi_{MD}$  was examined (Figure 2.3.14, 2.3.15). Relationships were found in the 2016 measurements, but not in the 2017 measurements. In 2016, K was positively related to  $\Psi_{PD}$  and  $\Psi_{MD}$ . However, water potential continued to decline after K was functionally zero. A regression was fit to K to examine the potential effect of throughfall reduction on the relationship between K and water potential as K declined to zero. There were no treatment differences detected in the slopes ( $K/\Psi_{PD}$ ,  $P = 0.459$ ;  $K/\Psi_{MD}$ ,  $P = 0.077$ ) or intercepts ( $K/\Psi_{PD}$ ,  $P = 0.352$ ;  $K/\Psi_{MD}$ ,  $P = 0.430$ ) of the relationships. Using data from both treatments, we found that for each 1.0 MPa decrease in  $\Psi_{PD}$ , we observed a  $2.1 \text{ mol m}^{-2} \text{ s}^{-1} \text{ MPa}^{-1}$  decrease in K ( $P = <0.001$ ;  $r^2 = 0.85$ ). Midday leaf water potential had less of an effect on K, as we found that for each 1.0 MPa decrease in  $\Psi_{MD}$ , we observed a  $1.6 \text{ mol m}^{-2} \text{ s}^{-1} \text{ MPa}^{-1}$  decrease in K ( $P = <0.001$ ;  $r^2 = 0.67$ ).

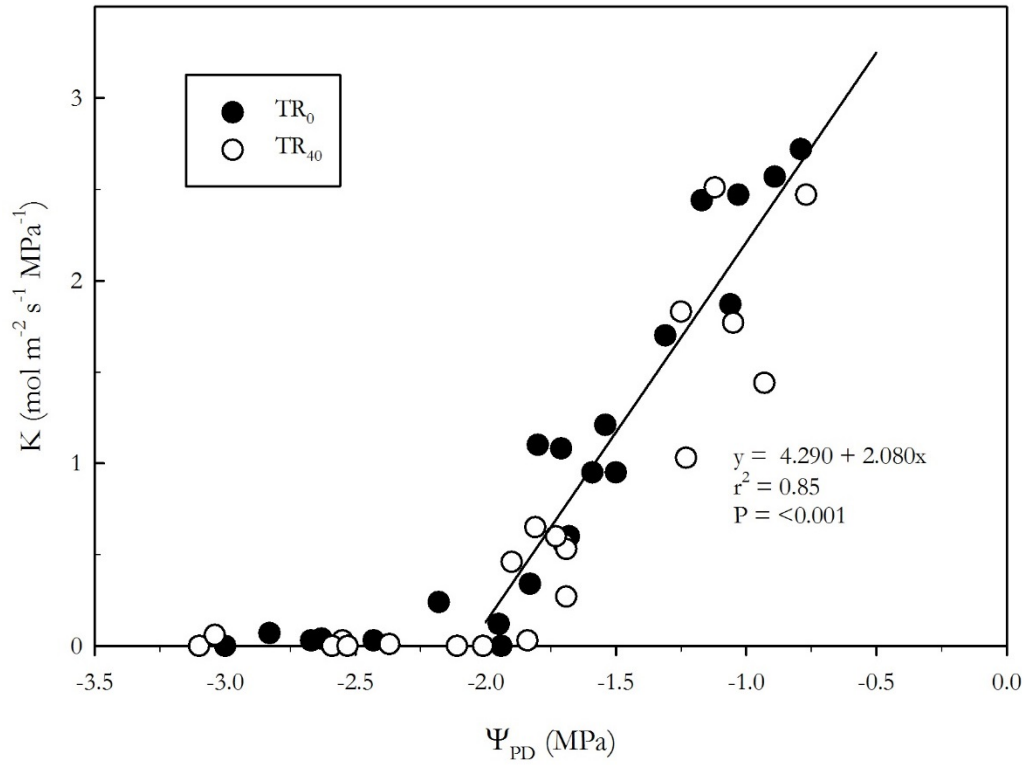


Figure 2.3.14. Whole-tree hydraulic conductance ( $K$ ) response to predawn water potential ( $\Psi_{PD}$ ) in a longleaf pine plantation in Marion County, Georgia measured from July 2016 through November 2016.

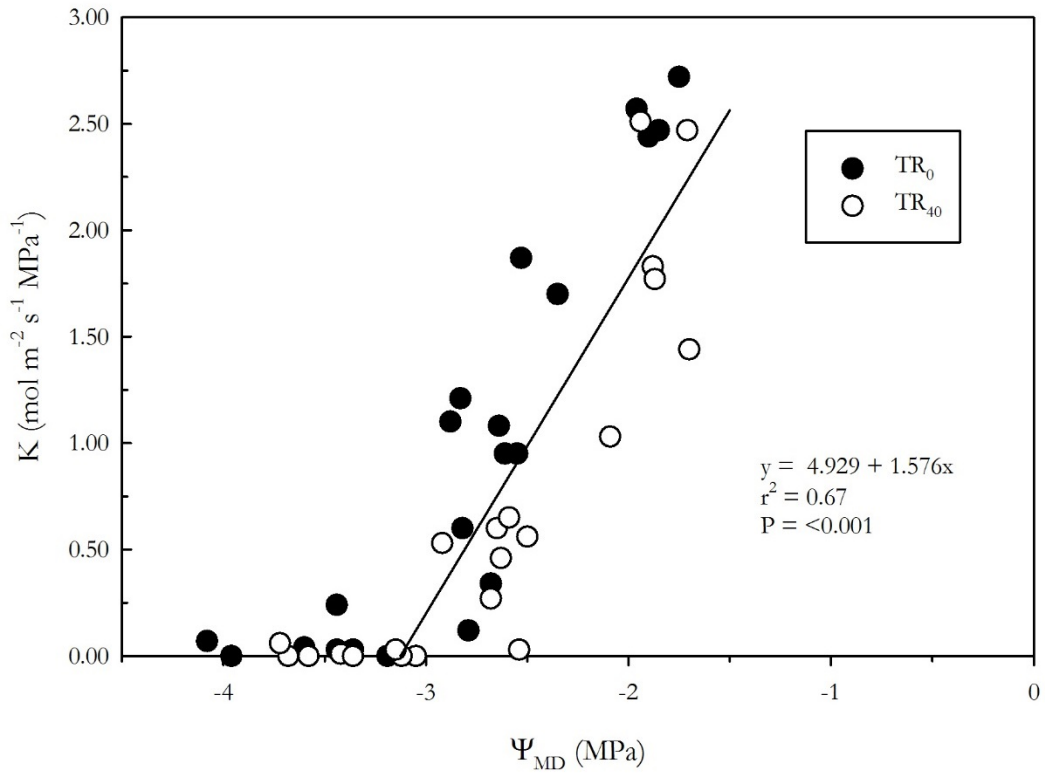


Figure 2.3.15. Whole-tree hydraulic conductance ( $K$ ) response to midday water potential ( $\Psi_{MD}$ ) in a longleaf pine plantation in Marion County, Georgia measured from July 2016 through November 2016.

### 2.3.6 Leaf $\delta^{13}\text{C}$ and Specific Leaf Area

Leaf  $\delta^{13}\text{C}$  did not differ between flushes or treatments, and no interaction between flush and treatment was detected for leaf  $\delta^{13}\text{C}$  (Table 2.3.1). Foliar N concentration was not different between flushes or between treatments, and no interaction transpired between flush and treatment. No differences were detected for needle length between treatments, but needles were 24.0% longer in the first flush than the second flush. A flush by treatment interaction occurred for specific leaf area. The effect of TR on SLA varied with flush. Treatment did not affect the SLA of the first flush ( $P = 0.306$ ). In the second flush  $\text{TR}_{40}$  increased the SLA from  $116.6 \text{ cm}^2 \text{ g}^{-1}$  to  $128.9 \text{ cm}^2 \text{ g}^{-1}$  ( $P = 0.003$ ), an increase of 10.5%.

Table 2.3.1. Mean (SE) foliar carbon-13 isotope composition ( $\delta^{13}\text{C}$ ), foliar nitrogen concentration (N), needle length, and specific leaf area (SLA) and observed probability values for two growing season flushes in response to throughfall treatment (TR;  $\text{TR}_0$ , ambient throughfall;  $\text{TR}_{40}$ , throughfall reduction) in a longleaf pine plantation in Marion County, Georgia measured in October 2016.

	$\delta^{13}\text{C}$ (‰)	Foliar N ( $\text{mg g}^{-1}$ )	Needle length (mm)	SLA ( $\text{cm}^2 \text{ g}^{-1}$ )
<b>Flush</b>				
1	-27.5 (0.2)	1.0 (0.03)	300.0 (5.8)	133.6 (0.1)
2	-27.2 (0.1)	1.0 (0.04)	242.0 (16.7)	122.8 (0.3)
<b>Throughfall treatment</b>				
$\text{TR}_0$	-27.5 (0.1)	1.0 (0.04)	283.3 (17.8)	124.4 (0.4)
$\text{TR}_{40}$	-27.3 (0.2)	1.0 (0.03)	258.6 (16.5)	132.0 (0.2)
<b>P &gt; F</b>				
Flush	0.446	0.800	<b>0.013</b>	<b>0.001</b>
TR	0.329	0.708	0.976	<b>0.005</b>
Flush x TR	0.390	0.451	0.617	<b>0.039</b>



### 2.3.7 LAI and Growth

No significant treatment effects occurred for basal area, density, DBH, or height (Table 2.3.2). Year had a significant effect on basal area, DBH, and height, with 2017 measurements being larger than 2016 measurements. Peak LAI was in August 2017 and was not different between treatments ( $P = 0.717$ ).

Table 2.3.2. Mean (SE) basal area, density, DBH, height, and maximum leaf area index (LAI) in August in response to throughfall treatment (TR; TR<sub>0</sub>, ambient throughfall; TR<sub>40</sub>, throughfall reduction) and observed probability values in a longleaf pine plantation in Marion County, Georgia.

	Basal area (m <sup>2</sup> ha <sup>-1</sup> )	Density (stems ha <sup>-1</sup> )	DBH (cm)	Height (m)	LAI (m <sup>2</sup> m <sup>-2</sup> )
<b>Year</b>					
2016	19.2 (0.9)	1000 (32)	15.4 (0.3)	10.3 (0.1)	-
2017	20.6 (0.8)	978 (33)	16.1 (0.3)	10.9 (0.2)	2.69 (0.09)
<b>Throughfall treatment</b>					
TR <sub>0</sub>	20.9 (1.1)	1029 (35)	15.8 (0.4)	10.8 (0.2)	2.73 (0.11)
TR <sub>40</sub>	19.0 (0.3)	949 (18)	15.7 (0.2)	10.4 (0.2)	2.65 (0.17)
<b>P&gt;F</b>					
Year	<b>0.002</b>	0.228	<b>&lt; 0.001</b>	<b>&lt; 0.001</b>	-
TR	0.288	0.221	0.867	0.157	0.717
Year x TR	0.898	0.670	0.265	0.316	-

## 2.4 Discussion

We captured longleaf pine's response to prolonged natural drought. In doing so, observed values showed that longleaf pine experiences lower  $\Psi_L$  than previously reported. Capturing the lower limits of  $\Psi_L$  allowed for a better understanding of where longleaf pine would be on the isohydric/anisohydric gradient. We also observed  $J_v$ ,  $J_\Sigma$ , and  $K$  as they decreased to near zero values in both the ambient and treatment plots as the drought persisted. Despite lowered transpiration during the 2016 drought, no growth differences in  $TR_0$  and  $TR_{40}$  were detected.

The trees in our study experienced extremely low water potentials during the 2016 natural drought. Under drought conditions and very low  $\theta$ , the  $\Psi_L$  measurements recorded at our study site were lower than  $\Psi_L$  reported in other studies. A study of mature (57-years-old on average) longleaf pine trees during drought in southwest Georgia reported  $\Psi_{PD}$  as low as -0.8 MPa and  $\Psi_{MD}$  as low as -1.7 MPa (Addington *et al.*, 2004). The study site in southwest Georgia was on a site similar to our study conditions, albeit with very different stand structure. Soils at the Addington *et al.* (2004) site were also Typic Quartzipsamment and experienced similarly low  $\theta$  ( $0.02 - 0.04 \text{ m}^3 \text{ m}^{-3}$ ) during the drought. However, the drought was shorter in duration than the drought that occurred in 2016, and the Addington *et al.* (2004) site experienced some relief in the form of intermediate (albeit low) precipitation events. The trees observed in the Addington *et al.* (2004) study were also older than our study trees, and would have had deeper and more established root systems with which to access water than the trees in our study. In another study of longleaf pine during drought, a 65-year-old mixed longleaf and slash pine (*Pinus elliottii* Engelm.) stand in northeast Florida,  $\Psi_L$  precipitation was <50% of historic averages (Gonzalez-Benecke *et al.*, 2011). Soil water potential (to which  $\Psi_{PD}$  is

analogous) was estimated at -0.96 MPa, while  $\Psi_{MD}$  was -1.83 MPa. Maggard et al. 2016 working with loblolly pine (*Pinus taeda* L.), found a 100% throughfall reduction decreased  $\theta$  to 4.8% and 15.6% at 0-12 cm and 12-45 cm depths respectively, decreasing  $\Psi_L$  to -1.3 MPa during predawn measurements and -1.9 MPa at midday. We observed  $\Psi_{PD}$  between -0.8 MPa and -3.2 MPa during the 2016 drought, values much lower than previously reported. The longleaf pine trees in our study also experienced much lower  $\Psi_{MD}$  (as low as -4.1 MPa) than were reported in other studies. The  $\Psi_L$  values are lower than the critical water potentials of other tree tissues where 50% loss of conductivity occurs. For example, in longleaf pine, 50% loss of conductivity occurs in roots at -1.31 MPa and in branches as -1.81 MPa (Gonzalez-Benecke *et al.*, 2010)

Across a season, Gonzalez-Benecke *et al.* (2011) reported a mean  $\Delta\Psi$  in longleaf pine of 0.94 MPa. We observed similar values of  $\Delta\Psi$ , except for the period at end of the drought in 2016 when  $\Delta\Psi$  declined sharply to 0.0 MPa and subsequently recovered.

We observed  $J_V$  values similar to other studies of longleaf pine. In longleaf pine on sandy soil in Georgia and Florida,  $J_V$  averaged 1.9 mol m<sup>-2</sup> s<sup>-1</sup> at midday in trees ranging from 35 cm to 42 cm in diameter (Ford *et al.*, 2004; Gonzalez-Benecke *et al.*, 2011). That value is similar to mean  $J_V$  values recorded in this study in 2017 (2.1 mol m<sup>-2</sup> s<sup>-1</sup> in TR<sub>0</sub>, 1.8 mol m<sup>-2</sup> s<sup>-1</sup> in TR<sub>40</sub>), but a great deal higher than values recorded in 2016 (0.9 mol m<sup>-2</sup> s<sup>-1</sup> in TR<sub>0</sub>, 0.6 mol m<sup>-2</sup> s<sup>-1</sup> in TR<sub>40</sub>), likely due to drought. We found that midday  $J_V$  was reduced relatively more during the 2016 drought year than in 2017. However, in both year TR<sub>40</sub> reduced average  $J_V$  by approximately 0.3 mol m<sup>-2</sup> s<sup>-1</sup>. The larger effect size in 2016 is likely because values were so low that any reduction would have a larger overall effect.

Trees in our study had higher rates of K during soil water deficit than other studies. Hydraulic conductance in longleaf pine has been estimated as approximately  $0.4 \text{ mol m}^{-2} \text{ s}^{-1} \text{ MPa}^{-1}$  when  $\theta$  at 50 cm depth was less than 10% (Addington *et al.*, 2004, 2006; Gonzalez-Benecke *et al.*, 2011). During 2016, at our site soil moisture at 50 cm was never above 6%, and average K values in TR<sub>0</sub> and TR<sub>40</sub> plots were near double that of other studies ( $0.7 \text{ mol m}^{-2} \text{ s}^{-1} \text{ MPa}^{-1}$  in TR<sub>40</sub> and  $1.0 \text{ mol m}^{-2} \text{ s}^{-1} \text{ MPa}^{-1}$  in TR<sub>0</sub>). The difference in K values may be due differences in the age and root profile of study trees, as Addington *et al.*, (2006) found that mature longleaf pine had a greater proportion of roots at depths below 50 cm than at shallower depths. In our study, we found that  $\Psi_{\text{PD}}$  was best explained by  $\theta_5$ , and that  $\Psi_{\text{PD}}$  began to respond to declining  $\theta_5$  at -1.7 MPa. Whole-tree hydraulic conductance values became similar to other studies once  $\Psi_{\text{PD}}$  decreased to around -1.9 MPa. It may be that younger trees are more sensitive to changes in  $\theta$  at shallow depths (where they have higher root concentrations) than mature trees, which will have established root systems at deeper depths.

We found that longleaf pine's response to prolonged drought was less isohydric than expected. When using classifications of isohydry/anisohydry that relate  $\Psi_{\text{MD}}$  and  $\Psi_{\text{PD}}$ , we found that longleaf pine was only partially isohydric ( $0 < \text{slope of } \Psi_{\text{MD}}/\Psi_{\text{PD}} < 1$ ) (Maritz-Vilalta *et al.*, 2014). In fact, with a slope of 0.85, longleaf pine is closer to a strictly anisohydric response (slope = 1), than a strictly isohydric response (slope = 0). Longleaf pine has been described as having an intermediate (in between isohydric and anisohydric) response to low  $\theta$  before, but previous observations had not reported as low  $\Psi_{\text{L}}$  as we observed (Gonzalez-Benecke *et al.*, 2011). Longleaf pine has a greater proportion of deep (below 0.6 m) roots and higher root to shoot ratio than other southern pine species, which might allow longleaf pine to better compete for water on xeric sites during severe drought (Gonzalez-Benecke *et al.*,

2011; Samuelson *et al.*, 2016). The lack of maintenance of  $\Psi_{MD}$  with declining  $\theta$  suggests that longleaf pine may benefit from continued carbon gain while avoiding fatal cavitation (Gonzalez-Benecke *et al.*, 2011). The carbon gains accumulated by longleaf pine during drought may contribute to improving access to belowground resources, potentially improving future drought resistance.

The water potential responses to declining  $\theta$  we observed did not follow the expected isohydric pattern. Midday water potential was not held constant as  $\theta$  decreased. The hypothesis that lower  $\theta$  due to drought will lower  $\Psi_{PD}$  and  $\Psi_{MD}$  was supported. During the 2016 measurement period,  $\Psi_{PD}$  was initially unresponsive to declining  $\theta_5$  but eventually declined when  $\theta_5$  reached 2.7%. Similarly,  $\Psi_{MD}$  did not respond until  $\theta_5$  was less than 4%. We also hypothesized that  $\Delta\Psi$  would be maintained as  $\Psi_{PD}$  declined, by stomatal control of  $\Psi_{MD}$ . That hypothesis was not supported, as we observed a significant effect of date on  $\Delta\Psi$  throughout the measurement period, indicating that  $\Delta\Psi$  was not consistent as water availability fluctuated. In typical isohydric behavior,  $\Delta\Psi$  should decrease as the soil dries and  $\Psi_{MD}$  becomes tightly regulated. If declines in  $K$  due to embolism are great enough, the  $\Delta\Psi$  response to declining soil moisture will become more isohydric (declining with soil moisture), behavior which was observed in this study during the end of the 2016 drought (Sperry, 2000; Roman *et al.*, 2015). Whole-tree hydraulic conductance declined as the 2016 season progressed, but  $\Delta\Psi$  was relatively unchanged until  $K$  declined to near-zero values in October.

Although drought has been shown to reduce growth in pine trees and increase susceptibility to mortality (Klos *et al.*, 2009), the hypothesis that  $TR_{40}$  would reduce aboveground growth was not supported. No treatment differences were detected for any growth variables, however drought effects may take years to impact mortality (Berdanier &

Clark, 2015). Longleaf pine growth is related to PDSI, particularly during the months when the worst of the 2016 drought occurred (Henderson & Grissino-Mayer, 2009). Drought may have limited transpiration and carbon accumulation enough in both treatments that no immediate growth changes were detected. Additionally, growth measurements began in July 2016, after much of the growing season had passed. Drought-related reductions in growth are dependent on the seasonal timing in which a drought occurs (Eilmann *et al.*, 2011). Because the natural drought occurred shortly after site establishment, an immediate baseline for growth rates was not available. We did not observe growth reductions, possibly because the majority of the year's growth may have occurred before the drought became severe. There were also no differences in LAI between treatments, so neither treatment had an advantage in carbon accumulation. Tree cores remain a viable option for future examination of site recovery following the end of the drought.

The hypothesis that TR<sub>40</sub> will cause slower recovery of  $J_V$  and  $K$  after natural drought also was not supported. No differences occurred in  $J_V$ ,  $J_\Sigma$ , or  $K$  as values were returning to observed 2016 maximums. However,  $J_\Sigma$  in 2017 suggests the TR<sub>40</sub> trees may be more sensitive to mild stress following the 2016 drought than TR<sub>0</sub> trees. After precipitation returned at the end of November 2016, there was no immediate difference in  $J_\Sigma$  between treatments. Once the increased stress of the 2017 summer came, TR<sub>40</sub> reduced average  $J_\Sigma$ . While not conclusive, this may be evidence of cumulative drought effects reducing  $J_\Sigma$  in TR<sub>40</sub>. Other evidence that TR<sub>40</sub> may have long-lasting effects on drought-related mortality is found in SLA. We found that TR<sub>40</sub> increased SLA by 10.5%. Increases in SLA could mean an increase in potential water use, and therefore increase in drought stress (Greenwood *et al.*, 2017). Higher SLA could also mean a reduction in photosynthetic machinery, and as there were no differences in needle

length between treatments, the increase in SLA is likely due to decreases in needle mass. If not recovered, reductions in photosynthetic machinery would lower the amount of accumulated carbon.

In summary, we examined the effect of a 40% throughfall reduction on water relations in a longleaf pine plantation. In 2016, the study area experienced a severe drought. Soil moisture,  $\Psi_L$ ,  $J_V$ ,  $J_\Sigma$ , and  $K$  decreased in both the ambient and treatment plots as the drought persisted. During the 2016 drought, the 40% throughfall reduction did not affect  $\Psi_L$  or  $J_\Sigma$ , but did reduce  $J_V$  and  $K$ . In 2017,  $J_V$  was reduced by  $TR_{40}$ , and  $J_\Sigma$  was also reduced on certain measurement days. We found that prolonged natural drought caused longleaf pine to behave less like a perfectly isohydric tree and more like an anisohydric tree. The partially isohydric behavior observed may allow longleaf pine to be more resistant to future drought stress and improve recovery.

## 2.5 Conclusions

Often during discussions of forest management and drought the focus is on large scale effects over large areas. However, because the conversation surrounding climate change and forests is about collections of individual organisms and not simply features on a landscape, it is important to understand the response of the individual to changes in its environment. Altering tree density to reallocate resources is a common tool of silviculture. Thinning decreases drought mortality risk (Dale *et al.*, 2001). To manage southeastern forests to be more resistant to climate changes, work done by Kerhoulas *et al.*, (2013) suggests a more intense thinning regimen beyond current practices is needed. Lower stand densities not only stimulate the growth of residual trees, but improve drought resilience if the treatment is timed appropriately (Kerhoulas *et al.*, 2013). However, a meta-analysis of drought mitigation through thinning that included sixteen studies on Pinus species (*P. taeda* L., *P. resinosa* Ait., *P. halepensis* Mill., *P. sylvestris* L., *P. nigra* Arnold, *P. ponderosa* Dougl. ex Laws, and *P. canariensis* C.Sm) showed that conifers' resistance to drought was not improved by thinning. Water use efficiency increased, but growth was reduced by 30 - 40%. Thinning increases crown diameter and creates larger rooting systems, increasing evaporative demand, which may offset the stand level benefit of lower tree density (Sohn *et al.*, 2016). Once the drought ended however, the large crowns and root systems of the conifers enabled tree growth to return pre-drought levels within a year, demonstrating the positive effects of thinning on conifer drought resilience. The Berdanier & Clark (2015) example highlights the importance of tree recovery to pre-disturbance levels for future drought survival.

In the Southeast US, managed forests are designed to be as uniform as site conditions will allow, and usually consist of one even-aged species. Pioneer species are used because they



are evolutionarily adapted to natural regeneration and grow easily in a nursery (Pretzsch & Forrester, 2017). While the simplicity of an even aged stand monoculture is what has allowed for many improvements in silviculture techniques over the last century (site index charts, stocking charts, growth and yield models), that simplicity is also a risk. Trees in a monoculture compete for the exact same nutritional and light level resources, so from a stand perspective there is little diversity in how resources are used (Klos *et al.*, 2009). High competition causes monoculture forests to be less resistant to drought stress than more species-rich forests, as different species use resources differently, lowering overall competition (Klos *et al.*, 2009). Increasing species mixture is a potential tool to insulate forests from effects of altered disturbance regimes. By selecting tree species that are more tolerant of drought and other climate-affected disturbances, a forest can be fortified against a wider range of disturbance scenarios (Dale *et al.*, 2001). However, managers are generally not changing their silvicultural practices (Keenan, 2015), and some researchers are suggesting that there isn't cause to alter conifer management in the southeastern United States (Coyle *et al.*, 2015). Temperate forests are at a relatively high risk to species range changes (Choat *et al.*, 2012), which may change management projections and make forestry fiscally unsustainable for some landowners. Diversifying managed forest areas presents opportunities for lower risk, but will require more intense management. Increasing species mix increases the complexity of silvicultural considerations needed to meet goals, and may be a cause for the lack of management changes (Pretzsch & Forrester, 2017). Traditional predictive tools often don't apply to mixed species forests, and interactions between species are often unknown (Pretzsch & Forrester, 2017).

Drought is a serious concern for the forested areas of the southeastern United States. Estimates of forest futures point towards more planted pine stands, which will likely be

loblolly pine, while existing diverse forests decline. Climate change threatens to increase temperatures and alter growing season precipitation patterns, which will test forests resistance and resilience as species respond to decreasing water availability. Longleaf pine may present a management solution, mitigating some effects of climate change through carbon sequestration. It will possibly be more resistant to drought-induced mortality than other southern pine species, and the research presented here suggests resiliency to extended periods of low water availability.

### 3 References

10HS Soil Moisture Sensor Manual. 2016.

**Addington RN, Donovan LA, Mitchell RJ, Vose JM, Pecot SD, B JS, Hacke UG, Sperry JS, Oren R. 2006.** Adjustments in hydraulic architecture of *Pinus palustris* maintain similar stomatal conductance in xeric and mesic habitats. *Plant, Cell and Environment* **29**: 535–545.

**Addington RN, Mitchell RJ, Oren R, Donovan LA. 2004.** Stomatal sensitivity to vapor pressure deficit and its relationship to hydraulic conductance in *Pinus palustris*. *Tree Physiology* **24**: 561–569.

**Allen CD, Macalady AK, Chenchouni H, Bachelet D, McDowell N, Vennetier M, Kitzberger T, Rigling A, Breshears DD, Hogg EH (Ted), et al. 2010.** A global overview of drought and heat-induced tree mortality reveals emerging climate change risks for forests. *Forest Ecology and Management* **259**: 660–684.

**Anderegg WRL, Klein T, Bartlett M, Sack L, Pellegrini AFA, Choat B, Jansen S. 2016.** Meta-analysis reveals that hydraulic traits explain cross-species patterns of drought-induced tree mortality across the globe. *Proceedings of the National Academy of Sciences* **113**: 5024–5029.

**Berdanier AB, Clark JS. 2015.** Multi-year drought-induced morbidity preceding tree death in Southeastern US forests. *Ecological Applications* **26**: 17–23.

**Boby L, Henderson J, Hubbard W. 2014.** The economic importance of forestry in the South - 2013. : 2.

**Boyer WD. 1990.** Longleaf Pine. Agricultural Handbook 654, Silvics of North America: 1. Conifers.819–836.

**Boyer JS. 1995.** Pressure Chamber. Measuring the Water Status of Plants and Soils. Academic Press, Inc., 13–48.

**Brodribb TJ. 2003.** Stomatal Closure during Leaf Dehydration, Correlation with Other Leaf Physiological Traits. *Plant Physiology* **132**: 2166–2173.

**Brodribb TJ, Cochard H. 2009.** Hydraulic Failure Defines the Recovery and Point of Death in Water-Stressed Conifers. *Plant Physiology* **149**: 575–584.

**Brodribb TJ, Hill RS. 2000.** Increases in Water Potential Gradient Reduce Xylem Conductivity in Whole Plants. Evidence from a Low-Pressure Conductivity Method. *Plant Physiology* **123**: 1021–1028.

**Čermák J, Kučera J, Nadezhdina N. 2004.** Sap flow measurements with some

thermodynamic methods, flow integration within trees and scaling up from sample trees to entire forest stands. *Trees* **18**: 529–546.

**Choat B, Jansen S, Brodribb TJ, Cochard H, Delzon S, Bhaskar R, Bucci SJ, Feild TS, Gleason SM, Hacke UG, et al. 2012.** Global convergence in the vulnerability of forests to drought. *Nature*: 4–8.

**Clark JS, Iverson L, Woodall CW, Allen CD, Bell DM, Bragg DC, D'Amato AW, Davis FW, Hersh MH, Ibanez I, et al. 2016.** The impacts of increasing drought on forest dynamics, structure, and biodiversity. *Global Change Biology* **22**: 17.

**Coyle DR, Klepzig KD, Koch FH, Morris LA, Nowak JT, Oak SW, Otrrosina WJ, Smith WD, Gandhi KJK. 2015.** A review of southern pine decline in North America. *Forest Ecology and Management* **349**: 134–148.

**Dale V, Joyce L, McNulty S, Neilson R, Ayres M, Flannigan M, Hanson P, Irland L, Lugo A, Peterson C, et al. 2001.** Climate change and forest disturbances. *BioScience* **51**: 723–734.

**Domec JC, Palmroth S, Ward E, Maier CA, ThÉrézien M, Oren R. 2009.** Acclimation of leaf hydraulic conductance and stomatal conductance of *Pinus taeda* (loblolly pine) to long-term growth in elevated CO<sub>2</sub> (free-air CO<sub>2</sub> enrichment) and N-fertilization. *Plant, Cell and Environment* **32**: 1500–1512.

**Eilmann B, Zweifel R, Buchmann N, Graf Pannatier E, Rigling A. 2011.** Drought alters timing, quantity, and quality of wood formation in Scots pine. *Journal of Experimental Botany* **62**: 2763–2771.

**Ford CR, McGuire MA, Mitchell RJ, Teskey RO. 2004.** Assessing variation in the radial profile of sap flux density in *Pinus* species and its effect on daily water use. *Tree Physiology* **24**: 241–249.

**Franks PJ, Drake PL, Froend RH. 2007.** Anisohydric but isohydrodynamic: Seasonally constant plant water potential gradient explained by a stomatal control mechanism incorporating variable plant hydraulic conductance. *Plant, Cell and Environment* **30**: 19–30.

**Frost C. 2006.** History and Future of the Longleaf. Pages: 9-48. *The Longleaf Pine Ecosystem*. 9–48.

**Garcia-Forner N, Adams HD, Sevanto S, Collins AD, Dickman LT, Hudson PJ, Zeppel MJB, Jenkins MW, Powers H, Martínez-Vilalta J, et al. 2016a.** Responses of two semiarid conifer tree species to reduced precipitation and warming reveal new perspectives for stomatal regulation. *Plant, Cell and Environment* **39**: 38–49.

**Garcia-Forner N, Biel C, Savé R, Martínez-Vilalta J. 2016b.** Isohydric species are not necessarily more carbon limited than anisohydric species during drought. *Tree Physiology* **37**: 441–455.

**Garcia-Forner N, Sala A, Biel Loscos C. 2015.** Individual traits as determinants of time of death under extreme drought in *P. sylvestris*. *New Phytologist*: 1–14.

**Gaylord ML, Kolb TE, McDowell NG, Meinzer F. 2015.** Mechanisms of piñon pine mortality after severe drought: A retrospective study of mature trees. *Tree Physiology* **35**: 806–

- Gilliam FS, Platt WJ. 1999.** Effects of long-term fire exclusion on tree species composition and stand structure in an old-growth *Pinus palustris* (Longleaf pine) forest. *Plant Ecology* **140**: 15–26.
- Gonzalez-Benecke CA, Martin TA, Cropper, WP. 2011.** Whole-tree water relations of co-occurring mature *Pinus palustris* and *Pinus elliottii* var. *elliottii*. *Canadian Journal of Forest Research* **41**: 509–523.
- Gonzalez-Benecke CA, Martin TA, Peter GF. 2010.** Hydraulic architecture and tracheid allometry in mature *Pinus palustris* and *Pinus elliottii* trees. *Tree Physiology* **30**: 361–375.
- Granier A. 1987.** Evaluation of transpiration in a Douglas-fir stand by means of sap flow measurements. *Tree Physiology* **3**: 309–20.
- Greenwood S, Ruiz-Benito P, Martínez-Vilalta J, Lloret F, Kitzberger T, Allen CD, Fensham R, Laughlin DC, Kattge J, Bönisch G, et al. 2017.** Tree mortality across biomes is promoted by drought intensity, lower wood density and higher specific leaf area. *Ecology Letters*: 539–553.
- Griffith GE, Omernik JM, Comstock JA, Lawrence S, Martin G, Goddard A, Hulcher VJ, Foster T. 2001.** *Ecoregions of Alabama and Georgia, (color poster with map, descriptive text, summary tables, and photographs):* Reston, Virginia,.
- Hanson PJ, Weltzin JF. 2000.** Drought disturbance from climate change: Response of United States forests. *Science of the Total Environment* **262**: 205–220.
- Henderson JP, Grissino-Mayer HD. 2009.** Climate–tree growth relationships of longleaf pine (*Pinus palustris* Mill.) in the Southeastern Coastal Plain, USA. *Dendrochronologia* **27**: 31–43.
- Hochberg U, Rockwell FE, Holbrook NM, Cochard H. 2017.** Iso/Anisohydry: A Plant–Environment Interaction Rather Than a Simple Hydraulic Trait. *Trends in Plant Science* **xx**: 1–9.
- Hodgson D, McDonald JL, Hosken DJ. 2015.** What do you mean, ‘resilient’? *Trends in Ecology and Evolution* **30**: 503–506.
- IPCC. 2013.** Atlas of Global and Regional Climate Projections. *Climate Change 2013: The Physical Science Basis. Contribution of Working Group I to the Fifth Assessment Report of the Intergovernmental Panel on Climate Change Annexe I*: 1311–1394.
- Jose S, Jokela EJ, Miller DL. 2006.** The Longleaf Pine Ecosystem. *The Longleaf Pine Ecosystem: Ecology, Silviculture, and Restoration*: 3–8.
- Kannenberg SA, Novick KA, Phillips RP. 2017.** Coarse roots prevent declines in whole-tree non-structural carbohydrate pools during drought in an isohydric and an anisohydric species. *Tree Physiology*: 1–9.
- Keenan RJ. 2015.** Climate change impacts and adaptation in forest management: a review. *Annals of Forest Science* **72**: 145–167.
- Kerhoulas LP, Kolb TE, Hurteau MD, Koch GW. 2013.** Managing climate change adaptation in forests: A case study from the U.S. Southwest. *Journal of Applied Ecology* **50**: 1311–1320.

- Klein T. 2014.** The variability of stomatal sensitivity to leaf water potential across tree species indicates a continuum between isohydric and anisohydric behaviours. *Functional Ecology* **28**: 1313–1320.
- Klos RJ, Wang GG, Bauerle WL, Rieck JR. 2009.** Drought Impact on Forest Growth and Mortality in the Southeast USA: An Analysis Using Forest Health and Monitoring Data. *Source: Ecological Applications Ecological Applications* **19**: 699–708.
- Lambers H, Stuart Chapin III F, Pons TL. 2008.** *Plant Physiological Ecology*.
- Lavoie-Lamoureux A, Sacco D, Risse PA, Lovisolo C. 2017.** Factors influencing stomatal conductance in response to water availability in grapevine: a meta-analysis. *Physiologia Plantarum* **159**: 468–482.
- Van Lear DH, Carroll WD, Kapeluck PR, Johnson R. 2005.** History and restoration of the longleaf pine-grassland ecosystem: Implications for species at risk. *Forest Ecology and Management* **211**: 150–165.
- Li W, Li L, Fu R, Deng Y, Wang H. 2007.** Changes to the North Atlantic Subtropical High and Its Impact on Summer Droughts / Floods in the Southeastern US Scientific Questions : *Journal of Climate* **24**: 1499–1506.
- Lu X, Kicklighter DW, Melillo JM, Reilly JM, Xu L. 2015.** United States : Regional- and state-level analyses. : 1–20.
- Lu P, Urban L, Zhao P. 2004.** Granier's Thermal Dissipation Probe (TDP) method for measuring sap flow in trees: Theory and practice. *Acta Bot. Sin.* **46**: 631–646.
- Maritz-Vilalta J, Poyatos R, Aguade D, Retana J, Mencuccini M. 2014.** A new look at water transport regulation in plants. *New Phytologist* **204**: 105–115.
- Martin T a., Brown KJ, Cermák J, Ceulemans R, Kucera J, Meinzer FC, Rombold JS, Sprugel DG, Hinckley TM. 1997.** Crown conductance and tree and stand transpiration in a second-growth *Abies amabilis* forest. *Canadian Journal of Forest Research* **27**: 797–808.
- Martínez-Vilalta J, Garcia-Forner N. 2016.** Water potential regulation, stomatal behaviour and hydraulic transport under drought: deconstructing the iso/anisohydric concept. *Plant, Cell & Environment*: 1–15.
- McDowell N, Pockman WT, Allen CD, Breshears DD, Cobb N, Kolb T, Plaut J, Sperry J, West A, Williams DG, et al. 2008.** Mechanisms of Plant Survival and Mortality during Drought : Why Do Some Plants Survive while Others Succumb to Drought? **178**: 719–739.
- McDowell NG, Ryan MG, Zeppel MJB, Tissue DT. 2013.** Feature: Improving our knowledge of drought-induced forest mortality through experiments, observations, and modeling. *New Phytologist* **200**: 289–293.
- McIntyre KR, Guldin JM, Ettl T, Ware C, Jones K. 2018.** Restoration of Longleaf Pine in the Southeastern United States: A Status Report. *Proceedings of the 19th biennial southern silvicultural research conference*: 297–302.
- Meinzer FC, Woodruff DR, Marias DE, Mcculloh KA, Sevanto S. 2014.** Dynamics of leaf water relations components in co-occurring iso- and anisohydric conifer species. *Plant, Cell and Environment* **37**: 2577–2586.

- Meinzer FC, Woodruff DR, Marias DE, Smith DD, McCulloh KA, Howard AR, Magedman AL. 2016.** Mapping ‘hydroscares’ along the iso- to anisohydric continuum of stomatal regulation of plant water status. *Ecology Letters* **19**: 1343–1352.
- Mitchell PJ, O’Grady AP, Pinkard EA, Brodribb TJ, Arndt SK, Blackman CJ, Duursma RA, Fensham RJ, Hilbert DW, Nitschke CR, et al. 2016.** An ecoclimatic framework for evaluating the resilience of vegetation to water deficit. *Global Change Biology* **22**: 1677–1689.
- Moore GW, Edgar CB, Vogel JG, Washington-Allen RA, March RG, Zehnder R. 2016.** Tree mortality from an exceptional drought spanning mesic to semiarid ecoregions. *Ecological Applications* **26**: 602–611.
- O’Brien MJ, Engelbrecht BMJ, Joswig J, Pereyra G, Schuldt B, Jansen S, Kattge J, Landhäusser SM, Levick SR, Preisler Y, et al. 2017.** A synthesis of tree functional traits related to drought-induced mortality in forests across climatic zones. *Journal of Applied Ecology* **54**: 1669–1686.
- Oishi AC, Hawthorne DA, Oren R. 2016.** Baseline: An open-source, interactive tool for processing sap flux data from thermal dissipation probes. *SoftwareX* **5**: 139–143.
- Oswalt CM, Cooper J a, Brockway DG, Brooks HW, Walker JL, Connor KF, Oswalt SN, Conner RC, Service USF. 2012.** History and Current Condition of Longleaf Pine in the Southern United States. : 60.
- Outcalt KW. 2000.** The longleaf pine ecosystem of the South. *Native Plants Journal* **1**: 42–53.
- Poyatos R, Aguadé D, Galiano L, Mencuccini M, Martínez-Vilalta J. 2013.** Drought-induced defoliation and long periods of near-zero gas exchange play a key role in accentuating metabolic decline of Scots pine. *New Phytologist* **200**: 388–401.
- Pretzsch H, Forrester DI. 2017.** *Mixed-Species Forests* (H Pretzsch, DI Forrester, and J Bauhus, Eds.). Springer Berlin Heidelberg.
- Roman DT, Novick KA, Brzostek ER, Dragoni D, Rahman F, Phillips RP. 2015.** The role of isohydric and anisohydric species in determining ecosystem-scale response to severe drought. *Oecologia* **179**: 641–654.
- Sala A, Piper F, Hoch G, The S, Phytologist N, April N, Baxter I, Hc P, Buchner P, Lahner B, et al. 2010.** Physiological mechanisms of drought-induced tree mortality are far from being resolved. *New Phytologist* **186**: 274–281.
- Salazar-Tortosa D, Castro J, Rubio De Casas R, Viñepla B, Sánchez-Cañete EP, Villar-Salvador P. 2018.** Gas exchange at whole plant level shows that a less conservative water use is linked to a higher performance in three ecologically distinct pine species. *Environmental Research Letters* **13**: 1–12.
- Samuelson LJ, Stokes TA, Butnor JR, Johnsen KH, Gonzalez-Benecke CA, Martin TA, Cropper WP, Anderson PH, Ramirez MR, Lewis JC. 2016.** Ecosystem carbon density and allocation across a chronosequence of longleaf pine forests in the southeastern USA. *Ecological Applications* **27**: 244–259.
- Seager R, Tzanova A, Nakamura J. 2009.** Drought in the Southeastern United States: Causes, variability over the last millennium, and the potential for future hydroclimate change.

*Journal of Climate* **22**: 5021–5045.

**Sheffield MCP, Gagnon JL, Jack SB, McConville DJ. 2003.** Phenological patterns of mature longleaf pine (*Pinus palustris* Miller) under two different soil moisture regimes. *Forest Ecology and Management* **179**: 157–167.

**Sohn JA, Saha S, Bauhus J. 2016.** Potential of forest thinning to mitigate drought stress: A meta-analysis. *Forest Ecology and Management* **380**: 261–273.

**Soil Survey Staff. 2016.** Web soil survey.

**Sperry JS. 2000.** Hydraulic constraints on plant gas exchange. *Agricultural and Forest Meteorology* **104**: 13–23.

**Sperry JS, Love DM. 2015.** What plant hydraulics can tell us about responses to climate-change droughts. *New Phytologist* **207**: 14–27.

**Starr G, Staudhammer CL, Wiesner S, Kunwor S, Loescher HW, Baron AF, Whelan A, Mitchell RJ, Boring L. 2016.** Carbon dynamics of *Pinus palustris* ecosystems following drought. *Forests* **7**: 1–25.

**Steppe K. 2018.** The potential of the tree water potential. *Tree Physiology* **38**: 937–940.

**Tardieu F, Simonneau T. 1998.** Variability among species of stomatal control under fluctuating soil water status and evaporative demand: modelling isohydric and anisohydric behaviours. *Journal of Experimental Botany*.

**Vandegehuchte MW, Steppe K. 2013.** Sap- flux density measurement methods : working principles and applicability. *Functional Plant Biology* **40**: 213–223.

**Wang H, Fu R, Kumar A, Li W. 2010.** Intensification of Summer Rainfall Variability in the Southeastern United States during Recent Decades. *Journal of Hydrometeorology* **11**: 1007–1018.

**Wear DN, Gries JG. 2013.** The Southern Forests Futures Project: Technical Report. *General Technical Report SRS-168* **1**.

**Wehner MF. 2004.** Predicted twenty-first-century changes in seasonal extreme precipitation events in the parallel climate model. *Journal of Climate* **17**: 4281–4290.

**Welles JM, Cohen S. 1996.** Canopy structure measurement by gap fraction analysis using commercial instrumentation. *Journal of Experimental Botany* **47**: 1335–1342.

**Will RE, Wilson SM, Zou CB, Hennessey TC. 2013.** Increased vapor pressure deficit due to higher temperature leads to greater transpiration and faster mortality during drought for tree seedlings common to the forest-grassland ecotone. *New Phytologist* **200**: 366–374.

**Wright JK, Williams M, Starr G, McGee J, Mitchell RJ. 2013.** Measured and modelled leaf and stand-scale productivity across a soil moisture gradient and a severe drought. *Plant, cell & environment* **36**: 467–83.

**Zweifel R, Rigling A, Dobbertin M. 2009.** Species-specific stomatal response of trees to drought - A link to vegetation dynamics? *Journal of Vegetation Science* **20**: 442–454.